ISSN 1846-6168 (Print), ISSN 1848-5588 (Online)
ID: TG-20161021143041

AN APPROXIMATE SOLUTION FOR THE PLANE WAVE DIFFRACTION BY AN IMPEDANCE STRIP: H-POLARIZATION CASE

OKVIRNO RJEŠENJE ZA DIFRAKCIJU RAVNOG VALA IMPEDACIJSKOM TRAKOM: SLUČAJ H-POLARIZACIJE

Emine Avşar Aydin, Turgut İkiz

Original scientific paper

Abstract: *In this study, the diffraction of H-polarized plane wave by an infinitely long strip which has the same impedance on both faces with a width of 2a is investigated by using an analytical-numerical method. The diffracted field is obtained by an integral equation in terms of the electric and magnetic currents induced by the incident field. This integral equation is reduced to two uncoupled integral equations that include only induced electric and magnetic currents separately. Both of the currents are defined as a sum of infinite series of Gegenbauer polynomials with unknown coefficients satisfying the edge conditions. The integral equations are transformed to linear algebraic equations by using analytical methods and the unknown coefficients are determined by solving numerically obtained matrix equations. Numerical examples on the RCS (radar cross section) are presented, and the far field scattering characteristics of the strip are discussed in detail. Some of the obtained results are compared with the other existing method.*

Keywords: *impedance, strip, analytic, numeric, diffraction*

Izvorni znanstveni članak

Sažetak: *U ovom radu istražuje se difrakcija H-polariziranog ravnog vala od beskonačno duge trake koja ima jednak otpor na obje strane i širinu 2a korištenjem analitičkog-numeričke metode. Difraktirano polje dobiveno je putem integralne jednadžbe u smislu električnih i magnetskih struja induciranih upadnim poljem. Ova integralna jednadžba svedena je na dvije odvojene integralne jednadžbe koje zasebno uključuju samo inducirane električne i magnetske struje. Obje struje definirane su kao zbroj beskonačnog niza Gegenbauerovih polinoma s nepoznatim koeficijentima koji zadovoljavaju rubne uvjete. Integralne jednadžbe pretvorene su u linearne algebarske jednadžbe pomoću analitičkih metoda i nepoznati su koeficijenti utvrđeni rješavanjem numerički dobivenih matričnih jednadžbi. Predstavljeni su numerički primjeri na PRP-u (površina radarskog presjeka), a karakteristike rasipanja na dalekom polju kod traka detaljno su raspravljeni. Neki od dobivenih rezultata uspoređeni su s drugom postojećom metodom.*

Ključne riječi: *impedacija, traka, analitički, numerički, difrakcija*

1. INTRODUCTION

The scattering of electromagnetic waves from geometrical and physical discontinuities is one of the most essential fields in the electromagnetic wave theory. However, the first considerable steps in this area of research are due to Lord Rayleigh and A.Sommerfeld. Almost a century ago, Rayleigh [39] (from Born M. [5]) investigated the problem of scattering by a perfectly conducting sphere; and Sommerfeld [45] overcame the problem of diffraction of plane electromagnetic waves by an absolutely conducting semi-infinite plane. Over the last few decades, the researches in the scattering of electromagnetic waves by several objects have been developed as a result of its direct applicability to civilian applications, including military ones, such as remote sensing, non-invasive diagnostics in medicine and non-destructive testing.

The received signal, which is spread by an object, can be used to resolve some of the geometrical and physical properties of the scatterer. Since the received scattered signal power is directly corresponds to the scattered field or radar cross section (RCS) of the object. Therefore, in military applications, in order to avoid the echo signal, the RCS of targets like air crafts must be cut down to a minimum level. Additionally, in order to decrease the inference caused by obstacle as buildings for instance, the RCS of such obstacles that are close to radars should also be reduced. Correspondingly, groups of engineers and scientists are also researching to extract as sufficient information as possible from low RCS values for both military and civilian applications.

Several methods exist, which are applicable to reduce the RCS of some obstacles. For instance, if the shape of the target is to be modified, scattered energy somehow may be directed toward some desired regions. But some other situations exist where shape modification is confined by the aerodynamic structure of that target, and another technique such as absorbing layer is applied for the same purpose. The absorber may consist of dielectric or magnetic materials, partially dielectric and/or magnetic materials or a number of layers of such materials. Even though such mixtures of shapes and materials propose more degrees of freedom in terms of design within controlling the RCS of the target, similarly, the complexity of the solution procedure is also increased.

Solutions for recognized problems including half-plane, cylinder or sphere are apparently essential regarding the diffraction theory, and strip is considered to be one of the most important familiar structures due to its geometry, strips are usually accustomed to investigate the multiple diffraction phenomenon. Furthermore, a large amount of applicable issues, especially in remote sensing, modeling by conducting, impedance or resistive strips is possible. Additionally, by using the duality principle diffracting a slit in an absolute conducting plane can be reduced to a perfectly conducting strip problem.

Scattering of cracks or gaps that may occur on the obstacle's surface, which is completely or partially filled with some material, may provide a significant contribution to the overall scattering pattern. In such issues the gaps or cracks may be modeled by strips and/or slits. Accordingly, due to its adjustment to many practical problems, strips have been broadly researched by many authors by using distinctive analytical and numerical strategies.

1.1. Literature Review

A large number of analytical techniques have been developed considering diffraction by scatterers with several shapes, sizes and constituent materials. These methods can be categorized in two groups, namely, exact and approximate methods. Using an exact method is possible, when the obstacle's geometry corresponds to a coordinate system having the wave equation separable.

Furthermore, exact solutions usually include sophisticated integral expressions, which are required to apply near-field, far-field or high-frequency asymptotic for engineering purposes. Due to these constraints not many practical problems have exact solutions, and mostly severe asymptotic expressions are acquired.

Approximate analytical techniques were obtained from the extension of classical optics by geometrical Theory of Diffraction (GTD) introduced by Keller [23] and Physical Theory of Diffraction (PTD) introduced by Ufimtsev (from Bhattacharyya. A.K. [4]).

In geometrical optics zero wavelength approximation is implemented and space is divided into distinct illuminated and shadow regions. It is considered that energy spreads in tube of rays, obviously the diffraction impacts are discarded in previous estimates; where these effects were first studied by GTD. At both incidence and reflection boundaries, the diffracted field becomes infinite and also at the edge which is caustic for the diffracted field. The term of a diffraction coefficient can be acquired simply by expressing the identical solution of a recognized problem in GTD form. In order to enhance GTD and overcome some of the methods' drawbacks two fundamental techniques have been developed namely, Uniform Asymptotic Theory of Diffraction (UAT) and Uniform Theory of Diffraction (UTD) introduced by Ahluwalia et.al [2] and Kouyoumjian and Pathak [24] respectively. In UAT it is considered that the field solution that occurs in an edge diffraction problem can be extended in a specific asymptotic series including a Fresnel integral, whereas in UTD Keller's diffraction, the coefficient is multiplied by a factor involving a Fresnel integral. The multiplication factor has a feature such that the field point approaches the shadow boundary and a finite field is obtained at the shadow boundaries while approaching zero.

In physical optics, surface currents are assumed to induce only at the illuminated part of the scatterer that functions as the supply of the scattered field. The accuracy of the technique can be raised by enhancing the assumed current distributions, however, it may not be able to account utterly for the presence of discontinuities on the obstacle. By PTD, Ufimtsev introduced the fringe current concept as a result of the physical or geometrical discontinuities. It was assumed that the entire current on a conducting surface includes a fringe current (nonuniform part) along with physical optics current. In distinction to GTD, PTD yields the finite fields everywhere including the shadow boundaries at the caustics.

Since its geometry is simple, the strip issue was researched by many scientists. Many techniques were proposed, but none yielded an efficient solution. So far, a severe solution for the problem of diffraction by a strip doesn't exist. However explaining the attempts to solve this problem which had yielded significant solutions, is worth it. Some of the considerations made will be given in a sequential order as follows.

Morse and Rubenstein [33] used a Mathieu function expansion for electromagnetic fields to obtain the exact series representation for the solution of the diffraction by strips. According to the rapid convergence of the Mathieu series, their solution yields improvement for low frequencies. However, when it comes to high frequency range their proposed method is not accurate since there is a necessity to include large number of terms while computing the infinite series.

Grinberg [16] proposed shadow current concept for diffraction issues regarding electromagnetic waves by a conducting slit by implementing the integral equation method. However, the same method could be applied to solve the problem of diffraction by a conducting strip, which is achieved by using the duality principle. The problem with this method is reduced to the solution of a second kind Fredholm equation. According to this formulation, the asymptotic form of the solution for the high frequency case can be obtained easily. It should be taken into account that the application of integral equation method have been used by other researches before Grinberg, in previous studies, e.g. Copson [12], Levine and Schwinger [27] and Miles [32]. Integral equation based formulation was firstly implemented by Copson [12] (from Senior, T.B.A. [42]) for a specific case of the Sommerfield half-plane which was an equation of the Wiener-Hopf type.

Up to 1950s, approximately all researches were focused on the diffraction by perfectly conducting structures. Senior [42] proposed the first study for the issue of finite conductivity, by using a semi-infinite metallic sheet as the diffracting structure. The stipulation used in this study was the standard impedance condition. For E-polarization, Senior defined two induced currents namely electric and magnetic, and by using Green's theory Senior had acquired the total field at any point off the plate in terms of these induced currents and incident field. The edge conditions for current components were being given as $O(x^{-1/2})$ and $O(x^{1/2})$ for $x \to 0$, for the tangential and normal components, respectively, of the electric and magnetic currents. The asymptotic behavior introduced by Senior [42] for the currents correspond to asymptotic behavior of the field components proposed by Meixner [31]. This is considered as one of the most essential information for our method. Accordingly, the information behind this behavior of currents at the edges give us the possibility to explain the currents in a series of some special functions with some unknowns.

It may be noted that the strip is used as a basic element in the formation of gratings. Diffraction by an impedance strip was researched by Faulkner [14] (from Bowman, J. J. [6]) via a Wiener-Hopf primarily based method, where the width of the strip was considered large compared to both the wavelength and the magnitude of the surface impedance such that it was being restricted to limited values. Maliuzhinets [28] (from Bowman. J. J. [6]) thought-out the wide strip drawback, furthermore, where the mutual interaction between the edges was neglected: then, the two edges were assumed as independent semi-infinite half planes, within the absence of the other being excited by an equivalent field alone.

Bowman [6] has also researched the high frequency back-scattering from an absorbing wide strip with random face impedances by using an approximation based on the known half plane solutions obtained by Maliuzhinets [28].

Multiple diffraction or the interaction among the diffracting edges of a strip is of great applicable importance additionally, diffraction problems which involve both slit and or strip geometry represent a three-part mixed boundary-value issue which strictly may be represented via triple integral equation approach that generally yields correspondingly to a modified Wiener-Hopf equation. Possibly, the solution for multiple diffractions are obtained by a repetitive procedure presented by Jones [22] (from Serbest A.H. and Büyükaksoy A. [44]). Kobayashi [25] had researched numerous types of modified Wiener-Hopf geometries and conjointly conferred the solution for H and E polarization cases. Another approximate method is presented by

Tiberio and Kouyoumjian [47] and is called extended spectral ray method which includes interpreting the incident field to the second edge as a sum of inhomogeneous plane waves that can be treated separately. By using this method, Herman and Volakis [18] had researched several diffraction by a conductive, resistive and impedance strips where the asymptotic solutions presented for these cases also involved the impacts of surface waves. The spectral iteration technique introduced by Büyükaksoy et al. [9] is considered an alternative spectral domain method furthermore, assuming that the edge is illuminated by the field diffracted from the other edge, it is possible to obtain the doubly diffracted field additionally, constructing another Wiener-Hopf problem for this configuration. A detailed discussion of the mentioned methods are given by Serbest and Büyükaksoy [44].

The development in numerical techniques for the solution of the scattering problems has always been parallel to the evolution in computer technology. Although numerical methods may be considered as more obvious compared to analytical methods, since the matrix inversion procedure for the analysis, computer capacity limits the size of the issue that can be dealt with. Generally, for the barriers having a maximum dimension of a few wavelengths, numerical methods are able to maintain precise solutions. The Method of Moments (MOM) and Galerkin's Method [17] are the popularly used numerical techniques. In MOM both the basic functions and the weighting functions are distinct however, they are considered similar functions in Galerkin's Method.

In numerical methods, the scattering drawbacks are presented as integral equations of both unknown field quantity and unknown induced surface current density by applying Green's theorem:

$$\vec{E}(\mathrm{r}) = -\frac{1}{4\pi}\int_s \begin{Bmatrix} i\omega\mu\left[\vec{n}\times\vec{H}\right]G(\mathrm{r},\mathrm{r}') \\ +\left[\vec{n}\times\vec{E}\right]\times\nabla G(\mathrm{r},\mathrm{r}') \\ +(\vec{n}.\vec{E})\nabla G(\mathrm{r},\mathrm{r}') \end{Bmatrix} ds \tag{1.1}$$

or in terms of surface current densities.

$$E(\mathrm{r}) = \mathrm{E}^i - \frac{i}{4}\int_s \{-iJ(\mathrm{r}') + M(\mathrm{r}')\frac{\partial}{\partial n}\}G(\mathrm{r},\mathrm{r}')\,\mathrm{ds} \tag{1.2}$$

The fundamental functions are broadly used for representing the currents on a given surface. However, in most studies the integral equation is achieved directly by applying the well-known methods such as Moment Method, Galerkin's Method or Finite Element Method.

Wandzura [53] investigated the current fundamental functions for curved surfaces in general. Volakis [52] researched the scattering by a narrow groove in an impedance plane, and solved the integral equations by presenting a single-basis study of the equivalent current on the narrow impedance insert. Based on these studies, the obtained integral equations are solved directly by applying either one of the above- mentioned numerical methods.

The GTD was used by Senior [43] to obtain the expression of the scattered field by a resistive strip where the results meet the ones obtained by the numerical solution of the integral equation including strips a narrow as a sixth of a wavelength. Senior also applied MOM to inspect the contribution of front and rear- edges to the far fields. it has been represented that, for strips with a width greater than about a half wavelength, the contribution regarding the front edge is similar to a half plane one, having similar resistance and the contribution of the rear edge is proportional to the square of the current at that point on the half plane corresponding to the rear edge of the strip.

Generally, the integral equations in Eq. (1.1) and Eq. (1.2) are usually solved by numerical methods However, they can also be reformed to a set of algebraic equations by applying some analytical techniques. Additionally, it is possible to solve the matrix equation obtained, by using standard matrix inversion algorithms. The time needed for the solution of this matrix equation is proportional to the size of the developed matrix. In the case of large bodies, the time required can be enormously large particularly for RCS estimation: Accordingly, the size of the matrix must be maintained as small as possible.

Emets and Rogowski [13] solved a two-dimensional problem of electromagnetic wave diffraction by a plane strip with different boundary conditions on its surfaces. The diffracted field was expressed by an integral in terms of the induced electric and magnetic current densities. The related boundary-value problem in the domain of the short-wavelength was occurred as a matrix Wienner-Hopf equation which was solved through the Khrapkov method. This analytical solution is a powerful tool to study the effects of a single strip under the incidence of plane waves. It can be used to validate the numerical methods.

Apaydın and Sevgi [3] studied on methods of moments (MoM) for modeling and simulation of scattered fields around infinite strip with one face soft and the other hard boundary conditions. Scattering cross-section was calculated numerically and compared with high-frequency asymptotics (HFA) models such as physical theory of diffraction (PTD) and theory of edge diffraction (TED). According to authors' knowledge, this method is the first application of MoM on the strip with one face soft and the other hard.

The H-polarized plane wave diffraction by a thin material strip has been solved using the Wiener-Hopf technique and approximate boundary conditions by Nagasaka and Kobayashi [34]. Employing a rigorous asymptotics, a high frequency solution for large strip width has been obtained. The numerical examples have been done on both the radar cross-section (RCS) and the far field scattering characteristics of the strip. Some of these examples have been compared with existing method and results agree reasonably well with existing method.

1.2. Comparison of Numerical-Analytical Methods

Commonly, the electrical size of the body restricts the tractability of numerical techniques, however, the geometrical complexity of the object restricts the applicability of the analytical methods. Furthermore, hybrid methods are used along with techniques based upon the extension of classical optics in order to obtain an asymptotic solution for problems regarding high region frequencies. Hybrid methods including both numerical and high frequency asymptotic techniques may have the ability to extend the class of electromagnetic scattering problems that can be handled.

The hybrid approach can be reformed as a field-based analysis where the GTD solution for the field associated with edge or surface diffraction are used as the initial point. These solutions function as the ansatz to the MoM formulation and represent the elements of a scatterer not meeting the requirements of a recognized geometry which is not cooperative with a GTD solution itself. (Burnside et.al. [7] and Sahalov and Thiele [41]). Alternatively, current-based formulation is possible in a situation such that the analysis proceeds from ansatz solutions for the currents obtained from physical optics and PTD (Thiele and Newhouse (1975), Ekelman and Thiele (1980) (from Medgyesi- Mitschang, L. N., 1989)) and Medgyesi-Mitschang and Wang (1983) (from Medgyesi- Mitschang, L. N., [29-30])). The option of a mixed field-current based approach also exists.

Generally, rigorous scattering theory, relies on the theory of boundary-value problems in which the progress is closely dependent, to mathematical branches. The main approach for the solution behind wave scattering is to reform the problem in terms of the integral equations satisfied by the unknown functions along with the current induced on the scatterer surface. Numerical techniques are utilized to shrink these integral equations to a system of linear algebraic equations. The presence of edges on the integration contour produce errors in current density calculations. In order to enhance the accuracy of the solution, some approaches accounting for the Meixner's edge condition in explicit form have been suggested by Shafai (1973) (from Veliev, I. E. [50]).

A similar technique was used by Butler [8] in which the analytical solution of the integral equation was obtained for the current induced on a confined conducting strip. In this solution the current mass was expressed as a product of a Chebyshev polynomial and a weighting operator which fulfill the edge condition and after specifying the Fourier type coefficients, the expression of far fields were obtained. So an integral equation which contains the current density and excitation was obtained as follows,

$$\begin{aligned} E_z^i(\mathrm{x}) = -j\frac{k\eta}{2\pi}\{ & \int_{-\infty}^{\infty} J_z(\mathrm{x}')\ln|x-x'|dx' \\ & +(\mathrm{c}+\ln\frac{k}{2})\int_{-\infty}^{\infty} J_z(\mathrm{x}')dx'\} \quad |x|\le\omega \end{aligned} \tag{1.3}$$

Where J_z is the unknown current density. $\eta=\sqrt{\mu/\varepsilon}$ and $c=\gamma+j(\pi/2)$, (c = 0.5772… is the Euler's constant). The solution for the current density was expressed as,

$$J_z(\mathrm{x}) = [1-(\frac{x}{\omega})^2]^{-1/2}\frac{f_0}{2}+\sum_{n=1}^{\infty} f_n T_n(\frac{x}{\omega}) \tag{1.4}$$

where $T(.)$ denotes the Chebyshev polynomials of the first kind and f_n's are the unknown coefficients. By using the orthogonality properties of the polynomials, the unknown coefficients and so the expression of the current density were obtained for both E and H-polarization cases.

A substitute technique was proposed by Veliev et al. [49-50] where the solution encompass any preassigned accuracy. The distributed field was represented using the Fourier transform of the corresponding surface current density which offers a number of enhancements to overcome the problem. A hybrid technique based on the semi-inversion procedure for equation operators and the method of moments was used to yield the optimal solution. The essentials of the solution and its application to the wave scattering by polygonal cylinders and flat conducting strip structures are proposed by Veliev and Veremey [49]. The previous versions of this method were suggested by (Nomura and Katsura [36], Hongo [19] and Otsuki [37] (from Veliev, E. I. [49])) for completely conducting strip and slit configurations. This analytical-numerical method, which utilizes spectral approach, somehow solves the problem to a system of linear algebraic equations for the unknown Fourier coefficients of the current density function. Appropriate truncation of the infinite system of equations can obtain the results with any desired accuracy.

It should be realized that the applicability of the truncation method cannot always be modified, additionally, the matrix elements correlated with the system of linear algebraic equations usually collapse slowly with an increase of their index.

1.3. Aims and the Scope of the Study

Despite there are various powerful analytical techniques, the main influence of numerical techniques is that they may be applied to a scatterer of random shape and are generally only restricted by the size of the scatterer. But this limitation is a realistic problem. Apparently, a set of linear equations which denote the scattering issue can be generated but the obtained set may be too large to be solved. Fortunately, the developments in computer technology make the solution of many electromagnetic problems possible for a required degree of accuracy. In contrast, the asymptotic techniques work best when compared to the wavelength the scatterer size is large .However, the difficulty of the problem increases when the complex shaped bodies are of interest.

The use of analytical methods along with numerical methods may bypass these restrictions. The numerical methods are limited to the bodies having a maximum dimension of less than a few wavelengths, while the analytical methods produce accurate outcomes for the scatterer much latter than those of one wavelength. Thereby, these methods may be combined to overcome the scattering problems involving scatterers of intermediate size and size in the resonance region. Additionally by using analytical-numerical methods the computation time required may be decreased to an acceptable level.

In this study, diffraction by an impedance strip is researched by using the analytical-numerical technique proposed by Veliev and Veremey [50]. In Chapter 2, the formulation of the problem for H-polarized raise is given. By expressing the electric and magnetic currents as infinite series in terms of Gegenbauer polynomials, two integral equations in spectral domain for electric and magnetic currents are derived. In Chapter 3, the integral equations are reduced to a system of linear algebraic equations for both currents with some unknown coefficients. In Chapter 4, some physical quantities are represented in terms of the unknown coefficients which will be denoted by solving the system of linear algebraic equations. In Chapter 5, the solution of branch-cut integrals are obtained and finally in Chapter 5, the curves for both currents, far field and RCS are represented. The results are reviewed and compared with some previously obtained results.

The aims of the current research are:

1 to employ a new analytical-numerical technique to solve a recognized diffraction problem that still does not have a proper solution,
2 to obtain an accurate solution for the impedance strip which can be used to simulate many practical obstacles,
3 to retrieve a solution which may work in a wide frequency range,
4 to set a base solution and write computer codes which may be used to analyze some complex structures that could be treated as a combination of multiple strips.

2. FORMULATION OF THE PROBLEM

The scatterer of the diffraction problem that will be formulated in this section is a strip of width $2a$ where the same impedance is assumed to be imposed on both sides. The geometry of the problem is illustrated in Figure 2.1 and η denotes the normalized impedance of the strip.

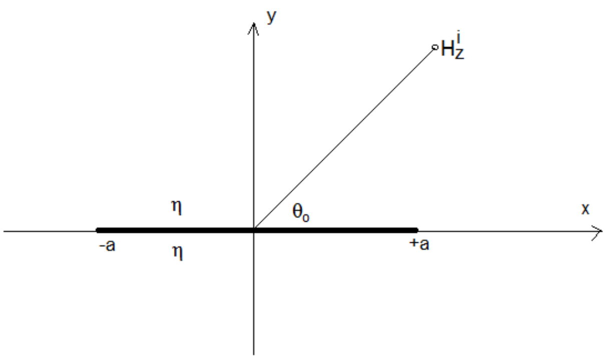

Figure 2.1. Geometry of the problem

Since the strip is uniform along the *z*-axis, the problem can be reduced to a two dimensional problem. The time dependence of the fields are assumed to be $\exp(-i\omega t)$ and suppressed throughout the analysis. The incident magnetic field is given as a linearly polarized plane wave

$$H_z^i(x,y) = e^{-ik(x\alpha_0 + y\sqrt{1-\alpha_0^2})} \tag{2.1}$$

where

$$\alpha_0 = cos\theta_0. \tag{2.2}$$

The total field is

$$H_z(x,y) = H_z^i(x,y) + H_z^s(x,y) \tag{2.3}$$

where H_z^s is the scattered field.

On the strip, the total field must satisfy the Leontovich boundary condition which is frequently called as impedance boundary condition, given by,

$$\left\{\frac{\partial H_z(x,y)}{\partial y} \pm ik\eta H_z(x,y)\right\}\Bigg|_{y=\pm 0} = 0. \tag{2.4}$$

So the total field can be expressed as [42]

$$H_z(x,y) = H_z^i(x,y) + \frac{1}{4}\int_{-a}^{a}\left\{kYI_m(x') - iI_e(x')\frac{\partial}{\partial y}\right\}. \quad H_0^{(1)}\left(k\sqrt{(x-x')^2+y^2}\right)dx \tag{2.5}$$

where I_m and I_e are the equivalent magnetic and electric current densities respectively. Expression of magnetic and electric current densities can be defined as follows respectively,

$$\overline{I_e} = \hat{a}_y \times \left[\overline{H}\right]_-^+ \qquad \left(\overline{H} = H\hat{a}_z\right) \tag{2.6}$$

$$\overline{I_e} = \hat{a}_y \times \left[\mathrm{H}_z(\mathrm{x},+0) - \mathrm{H}_z(\mathrm{x},-0)\right] \Rightarrow \tag{2.7}$$

$$\left[\mathrm{H}_z(\mathrm{x},+0) - \mathrm{H}_z(\mathrm{x},-0)\right]\hat{a}_x = f_2(\mathrm{x})\hat{a}_x$$

and

$$\overline{I_m} = \hat{a}_y \times \left[\overline{E}\right]_-^+ \tag{2.8}$$

$$i\omega\varepsilon_0\overline{E} = \nabla \times \overline{H} \qquad \overline{E} = \frac{1}{i\omega\varepsilon_0}\nabla \times \overline{H} \tag{2.9}$$

$$\overline{E} = \frac{1}{i\omega\varepsilon_0}\begin{pmatrix} \hat{a}_x & \hat{a}_y & \hat{a}_z \\ \frac{\partial}{\partial x} & \frac{\partial}{\partial y} & \frac{\partial}{\partial z} \\ 0 & 0 & H_z \end{pmatrix} \tag{2.10}$$

$$\overline{E} = \frac{1}{i\omega\varepsilon_0}\left\{\frac{\partial H_z}{\partial y}\hat{a}_x - \frac{\partial H_z}{\partial x}\hat{a}_y\right\} \tag{2.11}$$

$$\overline{I_m} = \frac{1}{i\omega\varepsilon_0}\left\{\frac{\partial H_z}{\partial y}\hat{a}_x - \frac{\partial H_z}{\partial x}\hat{a}_y\right\} \times \hat{a}_y \tag{2.12}$$

$$\overline{I_m} = \frac{1}{i\omega\varepsilon_0}\left\{\frac{\partial H(\mathrm{x},+0)}{\partial y} - \frac{\partial H(\mathrm{x},-0)}{\partial y}\right\}\hat{a}_z \tag{2.13}$$

$$kY = \omega\sqrt{\varepsilon_0\mu_0}\,.\,\frac{1}{Z} = \frac{\omega\sqrt{\varepsilon_0\mu_0}}{\sqrt{\frac{\mu_0}{\varepsilon_0}}} = \omega\varepsilon_0 \tag{2.14}$$

$$kY\overline{I_m} = \cancel{\omega\varepsilon_0}\left(\frac{1}{i\,\cancel{\omega\varepsilon_0}}\left\{\frac{\partial H(\mathrm{x},+0)}{\partial y} - \frac{\partial H(\mathrm{x},-0)}{\partial y}\right\}\right)\hat{a}_z$$
$$= -i\left\{\frac{\partial H(\mathrm{x},+0)}{\partial y} - \frac{\partial H(\mathrm{x},-0)}{\partial y}\right\}$$
$$= -if_1(\mathrm{x})\hat{a}_z$$

So Eq. 2.5 can be rearranged as

$$H_z(x,y) = H_z^i(x,y) - \frac{i}{4}\int_{-a}^{+a}\left\{f_1(x') + f_2(x')\frac{\partial}{\partial y}\right\}. \quad H_0^{(1)}(k\sqrt{(x-x')^2+y^2})dx' \tag{2.16}$$

2.1. Application of Boundary Conditions

If we rewrite the Leontovich boundary condition for $y = +0$ and $y = -0$, and if we subtract and add these two equations we can obtain the following expressions:

$$\frac{\partial H_z(\mathrm{x},+0)}{\partial y} + ik\eta H_z(\mathrm{x},+0) = 0 \tag{2.17}$$

and

$$\frac{\partial H_z(\mathrm{x},-0)}{\partial y} - ik\eta H_z(\mathrm{x},-0) = 0 \tag{2.18}$$

The difference of Eq. (2.17) and Eq. (2.18) is

$$\frac{\partial H_z(\mathrm{x},+0)}{\partial y} - \frac{\partial H_z(\mathrm{x},-0)}{\partial y} + ik\eta\left\{H_z(\mathrm{x},+0) + H_z(\mathrm{x},-0)\right\} = 0$$

(2.19)

And the sum is

$$\frac{\partial H_z(\mathrm{x},+0)}{\partial y} + \frac{\partial H_z(\mathrm{x},-0)}{\partial y} + ik\eta\left\{H_z(\mathrm{x},+0) - H_z(\mathrm{x},-0)\right\} = 0. \tag{2.20}$$

Using the expressions electric and magnetic current densities f_2 and f_1 in Eqs. (2.19) and (2.20)

$$f_1(\mathrm{x}) + \mathrm{i}k\eta\left\{H_z(\mathrm{x},+0) + H_z(\mathrm{x},-0)\right\} = 0 \tag{2.21}$$

$$f_2(\mathrm{x}) + \frac{1}{\mathrm{i}k\eta}\left\{\frac{\partial H_z(\mathrm{x},+0)}{\partial y} + \frac{\partial H_z(\mathrm{x},-0)}{\partial y}\right\} = 0 \tag{2.22}$$

are derived.

The expressions of total field at $y = \pm 0$ can be obtained from Eqs. (2.3) and (2.16) as

$$H_z(x,+0) = H_z^i(x,+0) - \lim_{y\to+0}\frac{i}{4}\int_{-a}^{+a}\left\{f_1(x') + f_2(x')\frac{\partial}{\partial y}\right\}. \quad H_0^1(k|x-x'|)dx' \tag{2.23}$$

and

$$H_z(x,-0) = H_z^i(x,-0) - \lim_{y\to-0}\frac{i}{4}\int_{-a}^{+a}\left\{f_1(x') + f_2(x')\frac{\partial}{\partial y}\right\}. \quad H_0^1(k|x-x'|)dx' \tag{2.24}$$

(2.15)

In Eq.(2.20), we require the sum of these two expressions as

$$H_z(x,+0)+H_z(x,-0)=$$
$$H_z^i(x,+0)+H_z^i(x,-0)$$
$$-\lim_{y\to+0}\frac{i}{4}\int_{-a}^{+a}\left\{f_1(x')+f_2(x')\frac{\partial}{\partial y}\right\}.H_0^1(k|x-x'|)dx' \quad (2.25)$$
$$-\lim_{y\to-0}\frac{i}{4}\int_{-a}^{+a}\left\{f_1(x')+f_2(x')\frac{\partial}{\partial y}\right\}.H_0^1(k|x-x'|)dx'.$$

For the incident field we have that

$$H_z^i(\mathrm{x},0)=H_z^i(\mathrm{x},+0)=H_z^i(\mathrm{x},-0)=e^{-ikx\alpha_0} \quad (2.26)$$

and from Senior [42] we have that

$$(\lim_{y\to+0}+\lim_{y\to-0})\int_{-a}^{+a}\left\{f_2(x')\frac{\partial}{\partial y}\right\}H_0^{(1)}(\mathrm{k}|x-x'|)\,\mathrm{dx}'=0 \quad (2.27)$$

and

$$\lim_{y\to+0}\int_{-a}^{+a}f_1(x')H_0^{(1)}(\mathrm{k}|x-x'|)\,\mathrm{dx}'=$$
$$\lim_{y\to-0}\int_{-a}^{+a}f_1(x')H_0^{(1)}(\mathrm{k}|x-x'|)\,\mathrm{dx}' \quad (2.28)$$
$$=\int_{-a}^{+a}f_1(x')H_0^{(1)}(\mathrm{k}|x-x'|)\,\mathrm{dx}'.$$

So by substituting Eq. (2.26) on Eq. (2.27) and Eq.(2.28) into Eq. (2.25) one can get that;

$$-\frac{1}{ik\eta}f_1(\mathrm{x})=2\,\mathrm{H}_z^i(\mathrm{x},0)-\frac{i}{2}\int_{-a}^{+a}f_1(x')H_0^{(1)}(\mathrm{k}|x-x'|)\,\mathrm{dx}' \quad (2.29)$$

or

$$-\frac{1}{k\eta}f_1(\mathrm{x})=2ie^{-ikx\alpha_0}+\frac{1}{2}\int_{-a}^{+a}f_1(x')H_0^{(1)}(\mathrm{k}|x-x'|)\,\mathrm{dx}' \quad (2.30)$$

Eq. (2.30) is the integral equation for the magnetic current $f_1(\mathrm{x})$.

At this stage we will derive the integral equation for magnetic current in spectral domain using the integral representation of Hankel function given as;

$$H_0^{(1)}(k|x-x'|)=\frac{1}{\pi}\int_{-\infty}^{+\infty}\frac{e^{ik(x-x')t}}{\sqrt{1-t^2}}dt. \quad (2.31)$$

Using Eq. (2.31) in Eq. (2.30)

$$-\frac{1}{k\eta}f_1(x)=2ie^{-ikx\alpha_0}+\frac{1}{2\pi}\int_{-a}^{+a}f_1(x')\int_{-\infty}^{+\infty}\frac{e^{ik(x-x')t}}{\sqrt{1-t^2}}dtdx' \quad (2.32)$$

and changing the order of integration

$$-\frac{1}{k\eta}f_1(x)=2ie^{-ikx\alpha_0}+\frac{1}{2\pi}\int_{-\infty}^{+\infty}\left\{\int_{-a}^{+a}f_1(x')e^{-ikx't}dx'\right\}\frac{e^{ikxt}}{\sqrt{1-t^2}}dt \quad (2.33)$$

is obtained. Where

$$F_1(t)=\int_{-a}^{+a}f_1(x')e^{-ikx't}dx' \quad (2.34)$$

is the Fourier transform of the magnetic current density $f_1(\mathrm{x})$. So

$$-\frac{1}{k\eta}f_1(x)=2ie^{-ikx\alpha_0}+\frac{1}{2\pi}\int_{-\infty}^{+\infty}F_m(t)\frac{e^{ikxt}}{\sqrt{1-t^2}}dt \quad (2.35)$$

is derived.

The following variable changes are required to be able to express the current density functions in terms of Gegenbauer polynomials.

Since $-a\le x\le a$, if we use the variable change $x=a\zeta,\quad x'=a\zeta',\quad \xi=ka$

$$F_1(t)=\int_{-1}^{+1}f_1(a\zeta')e^{-i(\xi/a)\mathrm{t}(a\zeta')}(ad\zeta') \quad (2.36)$$
$$F_1(t)=\int_{-1}^{+1}af_1(a\zeta')e^{-i\xi t\zeta'}d\zeta'$$

and let

$$\tilde{f}_1(\zeta')=af_1(a\zeta'). \quad (2.37)$$

So,

$$F_1(\mathrm{t})=\int_{-1}^{+1}\tilde{f}_1(\zeta')\,\mathrm{e}^{-i\xi t\zeta'}\,d\zeta' \quad (2.38)$$

is obtained. Means that Eq. (2.35) can be arranged as;

$$-\frac{1}{\left(\frac{\xi}{a}\right)\eta}f_1(x)=2ie^{-i\left(\frac{\xi}{a}\right)\alpha_0(a\zeta)}+\frac{1}{2\pi}\int_{-\infty}^{+\infty}F_m(t)\frac{e^{i\left(\frac{\xi}{a}\right)(a\zeta)t}}{\sqrt{1-t^2}}dt \quad (2.39)$$

or

$$-\frac{1}{\xi\eta}af_1(\mathrm{x})=2\,\mathrm{ie}^{-i\xi\alpha_0\zeta}+\frac{1}{2\pi}\int_{-\infty}^{+\infty}F_m(\mathrm{t})\frac{\mathrm{e}^{i\xi\mathrm{t}\zeta}}{\sqrt{1-t^2}}dt \quad (2.40)$$

and

$$-\frac{1}{\xi\eta}\tilde{f}_1(\zeta)=2ie^{-i\xi\alpha_0\zeta}+\frac{1}{2\pi}\int_{-\infty}^{+\infty}F_m(t)\frac{e^{i\xi t\zeta}}{\sqrt{1-t^2}}dt. \quad (2.41)$$

If we multiply both side of the equation by $e^{-i\xi\beta\zeta}$ and integrate between −1 and +1

$$-\frac{1}{\xi\eta}\int_{-1}^{1}\tilde{f}_1(\zeta)e^{-i\xi\beta\zeta}d\zeta=2i\int_{-1}^{1}e^{-i\xi\alpha_0\zeta}e^{-i\xi\beta\zeta}d\zeta+\frac{1}{2\pi}\int_{-1}^{1}e^{-i\xi\beta\zeta}\int_{-\infty}^{+\infty}F_m(t)e^{i\xi t\zeta}\frac{dt}{\sqrt{1-t^2}}d\zeta \quad (2.42)$$

is derived. From Eq. (2.33) it is obvious that the form on the left hand side can be expressed as

$$F_m(\beta)=\int_{-1}^{+1}\tilde{f}_1(\zeta)e^{-i\xi\beta\zeta}d\zeta. \tag{2.43}$$

The first term on the right hand side is

$$\int_{-1}^{+1}e^{-i\xi\alpha_0\zeta}e^{-i\xi\beta\zeta}d\zeta=2\frac{\sin\xi(\beta+\alpha_0)}{\xi(\beta+\alpha_0)} \tag{2.44}$$

and the second term on the right hand side by changing the order of integration;

$$\int_{-\infty}^{+\infty}\frac{F_m(t)}{\sqrt{1-t^2}}\int_{-1}^{1}e^{i\xi(t-\beta)\zeta}d\zeta dt=$$

$$\int_{-\infty}^{+\infty}\frac{F_m(t)}{\sqrt{1-t^2}}\left(\frac{e^{i\xi(t-\beta)\zeta}}{i(t-\beta)\xi}\right)\Bigg|_{-1}^{1}dt \tag{2.45}$$

$$=\frac{2}{\xi}\int_{-\infty}^{+\infty}\frac{F_m(t)}{\sqrt{1-t^2}}\frac{\sin\xi(t-\beta)}{(t-\beta)}dt$$

is obtained. So Eq. (2.41) can be rearranged as

$$-\frac{1}{\xi\eta}F_m(\beta)=4i\frac{\sin\xi(\beta+\alpha_0)}{\xi(\beta+\alpha_0)}+\frac{1}{\xi\pi}\int_{-\infty}^{+\infty}\frac{F_m(t)}{\sqrt{1-t^2}}\frac{\sin\xi(t-\beta)}{t-\beta}dt. \tag{2.46}$$

This equation is the integral equation for the magnetic current density in spectral domain. In a similar way, the integral equation for the electric current density in spectral domain is obtained. This equation can be expressed as

$$F_e(\beta)=\frac{4}{\eta}\sqrt{1-{\alpha_0}^2}\frac{\sin\xi(\beta+\alpha_0)}{\xi(\beta+\alpha_0)}-\frac{1}{\pi\eta}\int_{-\infty}^{\infty}F_e(\mathrm{t})\sqrt{1-t^2}\frac{\sin\xi(\mathrm{t}-\beta)}{\mathrm{t}-\beta}dt \tag{2.47}$$

3. REDUCTION OF LINEAR EQUATIONS TO THE SYSTEM OF LINEAR ALGEBRAIC EQUATIONS

In this section, the solution of the integral for electric $F_e(\beta)$ and magnetic $F_m(\beta)$ current densities will be reduced to the solution of two uncoupled system of linear algebraic equations. The first step of the reduction process is to express the current densities in Fourier transform domain and obtain a general spectral expression for currents. Then by using the constraints implied by edge conditions, electric and magnetic current density expressions will be obtained in transform domain. Finally, they will be written in the form of infinite system of linear algebraic equations involving Gegenbauer polynomial coefficients as unknowns.

3.1. General Expressions for the Current Density Functions in the Transform Domain

Since it is necessary to express the current functions in spectral domain, the Fourier transform $F(\beta)$ of the current density function $\tilde{f}(\zeta)$ must be found as

$$F(\beta)=\int_{-1}^{+1}\tilde{f}(\zeta)e^{-i\xi\beta\zeta}d\zeta. \tag{3.1}$$

The current density function $\tilde{f}(\zeta)$ is defined for $|\zeta|\le 1$ and it is zero elsewhere. Let $\tilde{f}(\zeta)$ be represented by a uniformly convergent series, such as,

$$\tilde{f}(\zeta)=(1-\zeta^2)^{\upsilon}\sum_{n=0}^{\infty}f_nC_n^{\upsilon+\frac{1}{2}}(\zeta) \tag{3.2}$$

where $C_n^{\upsilon+\frac{1}{2}}(\zeta)$ denote the Gegenbauer polynomials and υ is a constant related to the edge condition. The value of υ in Eq. (3.2) will be determined by enforcing the functions such as to satisfy the edge conditions for electric and magnetic current densities separately.

For the electric current density function $\tilde{f}_e(\zeta)$, and the magnetic current density function $\tilde{f}_m(\zeta)$, from Meixner's (1972) edge conditions, v can be determined for $\zeta\to 0$ as,

$$\tilde{f}_e(\zeta)=O(\zeta^{-1/2})\ \ and\ \ \tilde{f}_m(\zeta)=O(\zeta^{1/2}). \tag{3.3}$$

The order relations given above for electric and magnetic current densities can be obtained respectively as $\upsilon=-1/2$ and $\upsilon=1/2$ by considering the asymptotic behavior of Gegenbauer polynomials together with Eq. (3.2). The integration in Eq. (3.1) is divided into two parts, as follows

$$F(\beta)=\int_{-1}^{0}\tilde{f}(\zeta)e^{-i\xi\beta\zeta}d\zeta+\int_{0}^{+1}\tilde{f}(\zeta)e^{-i\xi\beta\zeta}d\zeta \tag{3.4}$$

By replacing ζ with $-\zeta$ and by changing the order of upper and lower limits in the first term on the right-hand-side, Eq. (3.4) will be written as:

$$F(\beta)=\int_{0}^{1}\tilde{f}(-\zeta)e^{-i\xi\beta\zeta}d\zeta+\int_{0}^{1}\tilde{f}(\zeta)e^{-i\xi\beta\zeta}d\zeta. \tag{3.5}$$

Now to determine $\tilde{f}(-\zeta)$ the following formula (Prodnikov, A. P., 1983, p. 732) will be used

$$C_n^{\lambda}(-\mathrm{z})=(-1)^nC_n^{\lambda}(\mathrm{z}) \tag{3.6}$$

and, $\tilde{f}(-\zeta)$ can be expressed as:

$$\tilde{f}(-\zeta)=(1-\zeta^2)^{\upsilon}\sum_{n=0}^{\infty}(-1)^n f_n C_n^{\upsilon+\frac{1}{2}}(\zeta). \tag{3.7}$$

By substituting Eqs. (3.7) and (3.2) into Eq. (3.5),

$$F(\beta)=\int_{0}^{+1}(1-\zeta^2)^{\upsilon}\sum_{n=0}^{\infty}f_n C_n^{\upsilon+\frac{1}{2}}(\zeta).\left\{e^{-i\xi\beta\zeta}+(-1)^ne^{i\xi\beta\zeta}\right\}d\zeta \tag{3.8}$$

is obtained. If *n* is even, i.e. *n* = 2*p*, then Eq. (3.8) takes the form of,

$$F_{ev}(\beta)=2\int_0^{+1}(1-\zeta^2)^{\upsilon}\sum_{p=0}^{\infty}f_{2p} .C_{2p}^{\upsilon+\frac{1}{2}}(\zeta)\left\{\frac{e^{-i\xi\beta\zeta}+e^{i\xi\beta\zeta}}{2}\right\}d\zeta \tag{3.9}$$

or

$$F_{ev}(\beta)=2\int_0^{+1}(1-\zeta^2)^{\upsilon}\sum_{p=0}^{\infty}f_{2p} .C_{2p}^{\upsilon+\frac{1}{2}}(\zeta)\cos(\xi\beta\zeta)\,d\zeta. \tag{3.10}$$

By changing the order of integration and summation

$$F_{ev}(\beta)=2\sum_{p=0}^{\infty}f_{2p}K_{2p} \tag{3.11}$$

is written with

$$K_{2p}=\int_0^{+1}(1-\zeta^2)^{\upsilon}C_{2p}^{\upsilon+\frac{1}{2}}(\zeta)\cos(\xi\beta\zeta)\,d\zeta\,. \tag{3.12}$$

On the other hand, if n is odd, i.e. $n = 2p+1$ then Eq. (3.8) takes the form of,

$$F_{od}(\beta)=\int_0^{+1}(1-\zeta^2)^{\upsilon}\sum_{p=0}^{\infty}f_{2p+1} .C_{2p+1}^{\upsilon+\frac{1}{2}}(\zeta)\,2\mathrm{i}\left\{\frac{e^{-i\xi\beta\zeta}-e^{i\xi\beta\zeta}}{2i}\right\}d\zeta \tag{3.13}$$

or

$$F_{od}(\beta)=-2i\int_0^{+1}(1-\zeta^2)^{\upsilon}\sum_{p=0}^{\infty}f_{2p+1} .C_{2p+1}^{\upsilon+\frac{1}{2}}(\zeta)\sin(\xi\beta\zeta)d\zeta. \tag{3.14}$$

Again by changing the order of integration and summation, it yields

$$F_{od}(\beta)=-2i\sum_{p=0}^{\infty}f_{2p+1}K_{2p+1} \tag{3.15}$$

with

$$K_{2p+1}=\int_0^{+1}(1-\zeta^2)^{\upsilon}C_{2p+1}^{\upsilon+\frac{1}{2}}(\zeta)\sin(\xi\beta\zeta)d\zeta\,. \tag{3.16}$$

It can easily be seen from Eq. (3.8) that,

$$F(\beta)=F_{ev}(\beta)+F_{od}(\beta) \tag{3.17}$$

Now, in order to express K_{2p} and K_{2p+1} in a form convenient for numerical calculations, the following expressions [38] are being used:

$$\int_0^1(1-\mathrm{x}^2)^{z-\frac{1}{2}}C_{2n+1}^{z}(\mathrm{x})\sin(\mathrm{ax})\,\mathrm{dx}= (-1)^n\pi\frac{\Gamma(2\mathrm{n}+2\mathrm{z}+1)J_{2n+z+1}(\mathrm{a})}{(2\mathrm{n}+1)!\,\Gamma(\mathrm{z})\,(2\mathrm{a})^z} \tag{3.18}$$

$$\int_0^1(1-\mathrm{x}^2)^{z-\frac{1}{2}}C_{2n}^{z}(\mathrm{x})\cos(\mathrm{ax})\,\mathrm{dx}= (-1)^n\pi\frac{\Gamma(2\mathrm{n}+2\mathrm{z})J_{2n+z}(\mathrm{a})}{(2\mathrm{n})!\,\Gamma(\mathrm{z})\,(2\mathrm{a})^z}. \tag{3.19}$$

As usual, $\Gamma(.)$ denotes the Gamma functions and $J_n(.)$ denotes the well-known Bessel function of the first kind. In Eqs. (3.18) and (3.19), by setting $x=\zeta, z=\upsilon+\frac{1}{2}$ and $a=\xi\beta$, the followings can be written

$$K_{2p}=\int_0^{+1}(1-\zeta^2)^{\upsilon}C_{2p}^{\upsilon+\frac{1}{2}}(\zeta)\cos(\xi\beta\zeta)\,\mathrm{d}\zeta= (-1)^p\frac{\Gamma(2p+2\upsilon+1)J_{2p+\upsilon+\frac{1}{2}}(\xi\beta)}{(2p)!\,\Gamma(\upsilon+\frac{1}{2})\,(2\xi\beta)^{\upsilon+\frac{1}{2}}} \tag{3.20}$$

and

$$K_{2p+1}=\int_0^{+1}(1-\zeta^2)^{\upsilon}C_{2p+1}^{\upsilon+\frac{1}{2}}(\zeta)\sin(\xi\beta\zeta)\,\mathrm{d}\zeta= (-1)^p\pi\frac{\Gamma(2p+2\upsilon+2)J_{2p+\upsilon+\frac{3}{2}}(\xi\beta)}{(2p+1)!\,\Gamma(\upsilon+\frac{1}{2})\,(2\xi\beta)^{\upsilon+\frac{1}{2}}}. \tag{3.21}$$

From Eq. (3.11), Eq. (3.15) and Eq. (3.17) $F(\beta)$ is

$$F(\beta)=2\sum_{p=0}^{\infty}f_{2p}K_{2p}-2i\sum_{p=0}^{\infty}f_{2p+1}K_{2p+1} \tag{3.22}$$

and from Eqs. (3.20) and (3.21), it can be written as

$$\begin{aligned}F(\beta)=&\,2\sum_{p=0}^{\infty}f_{2p}(-1)^p\pi .\frac{\Gamma(2\mathrm{p}+2\upsilon+1)}{\Gamma(2\mathrm{p}+1)}\frac{J_{\upsilon+\frac{1}{2}+2p}(\xi\beta)}{\Gamma(\upsilon+\frac{1}{2})(2\xi\beta)^{\upsilon+\frac{1}{2}}}\\&-2i\sum_{p=0}^{\infty}f_{2p+1}(-1)^p\pi .\frac{\Gamma(2\mathrm{p}+2\upsilon+2)}{\Gamma(2\mathrm{p}+2)}\frac{J_{\upsilon+\frac{3}{2}+2p}(\xi\beta)}{\Gamma(\upsilon+\frac{1}{2})(2\xi\beta)^{\upsilon+\frac{1}{2}}}\end{aligned} \tag{3.23}$$

or

$$F(\beta)=\frac{2\pi}{\Gamma(\upsilon+\frac{1}{2})}\sum_{p=0}^{\infty}(-1)^p .\left\{f_{2p}\frac{\Gamma(2\mathrm{p}+2\upsilon+1)}{\Gamma(2\mathrm{p}+1)}\frac{J_{\upsilon+\frac{1}{2}+2p}(\xi\beta)}{(2\xi\beta)^{\upsilon+\frac{1}{2}}} -i\,f_{2p+1}\frac{\Gamma(2\mathrm{p}+2\upsilon+2)}{\Gamma(2\mathrm{p}+2)}\frac{J_{\upsilon+\frac{3}{2}+2p}(\xi\beta)}{(2\xi\beta)^{\upsilon+\frac{1}{2}}}\right\}. \tag{3.24}$$

By rearranging the last equation, the Fourier transform of the current density function can be obtained as follows:

$$F(\beta)=\frac{2\pi}{\Gamma(\upsilon+\frac{1}{2})}\sum_{n=0}^{\infty}(-i)^n f_n \cdot\frac{\Gamma(\mathrm{n}+2\upsilon+1)}{\Gamma(\mathrm{n}+1)}\frac{J_{n+\upsilon+\frac{1}{2}}(\xi\beta)}{(2\xi\beta)^{\upsilon+\frac{1}{2}}}. \quad (3.25)$$

This completes the calculation for the Fourier transform of a current element represented in terms of Gegenbauer polynomials given by Eq. (3.2). Since no restriction is imposed on the current series expression during the derivation, it is obvious that this representation is valid for both electric and magnetic currents.

Now considering the edge conditions separately for electric and magnetic current components, the corresponding spectral expressions in the Fourier domain can easily be obtained. First, the magnetic current density will be obtained simply by substituting $\upsilon=1/2$ which yields

$$F_m(\beta)=\pi\sum_{n=0}^{\infty}(-\mathrm{i})^n(\mathrm{n}+1)\ f_n^m\frac{J_{n+1}}{\xi\beta}. \quad (3.26)$$

Similarly, by inserting $\upsilon=-1/2$ in Eq. (3.25) it is possible to obtain the Fourier transform of the electric current density. But, it is obviously seen that due to the presence of $\left[\Gamma(\upsilon+1/2)\right]^{-1}$ term in the expression, the current density will have a singularity in this case. Therefore, in order to remove this singularity the series expansion given by Eq. (3.2) will be used for $\upsilon=-1/2$:

$$\tilde{f}_e(\zeta)=(1-\zeta^2)^{-\frac{1}{2}}\sum_{n=0}^{\infty}f_n^e\,\mathrm{C}_n^0(\zeta). \quad (3.27)$$

In [38] it is given that,

$$\mathrm{C}_n^0(\zeta)=\frac{2}{n}T_n(\zeta) \quad (3.28)$$

where $\mathrm{T}_n(.)$ denotes the well-known Chebyshev polynomials which is valid for $n\neq 0$; therefore, Eq. (3.27) can be written as,

$$\tilde{f}_e(\zeta)=(1-\zeta^2)^{-\frac{1}{2}}\sum_{n=0}^{\infty}f_n^e\ \frac{2}{n}T_n(\zeta). \quad (3.29)$$

From Eq. (3.1), the Fourier transform of $\tilde{f}(\zeta)$ for $\upsilon=-\frac{1}{2}$ is,

$$F_e(\beta)=\int_{-1}^{+1}(1-\zeta^2)^{-\frac{1}{2}}\sum_{n=1}^{\infty}f_n^e\ \frac{2}{n}T_n(\zeta)\ e^{-i\xi\beta\zeta}d\zeta \quad (3.30)$$

or

$$F_e(\beta)=\sum_{n=1}^{\infty}\frac{2}{n}f_n^e\int_{-1}^{+1}(1-\zeta^2)^{-\frac{1}{2}}\ T_n(\zeta)\ e^{-i\xi\beta\zeta}d\zeta\ . \quad (3.31)$$

The following equality is given for $n\neq 0$ in [38]

$$\int_{-a}^{a}\frac{1}{\sqrt{a^2-x^2}}T_n\left(\frac{x}{a}\right)e^{ipx}dx=i^n\pi J_n(\mathrm{ap}) \quad (3.32)$$

so the integral in Eq. (3.31) can be calculated as,

$$\int_{-1}^{1}(1-\zeta^2)^{-\frac{1}{2}}T_n\left(\zeta\right)e^{-i\xi\beta\zeta}d\zeta=\pi(-\mathrm{i})^n J_n(\xi\beta) \quad (3.33)$$

and by substituting Eq. (3.33) into Eq. (3.31),

$$F_e(\beta)=\pi\sum_{n=1}^{\infty}(-\mathrm{i})^n\frac{2}{n}f_n^e J_n(\xi\beta) \quad (3.34)$$

is obtained.

Now, in order to calculate the contribution for n = 0, let the analysis start with the series expansion for the Fourier transform of the current given by Eq. (3.25):

$$F(\beta)=\frac{2\pi}{\Gamma(\upsilon+\frac{1}{2})}\sum_{n=0}^{\infty}(-i)^n f_n \cdot\frac{\Gamma(\mathrm{n}+2\upsilon+1)}{\Gamma(\mathrm{n}+1)}\frac{J_{\mathrm{n}+\upsilon+\frac{1}{2}}(\xi\beta)}{(2\xi\beta)^{\upsilon+\frac{1}{2}}}.$$

The term $\Gamma(\mathrm{n}+2\mathrm{v}+1)$ can be written in a more convenient form:

$$\Gamma(\mathrm{n}+2\upsilon+1)=\Gamma(\mathrm{n}+2(\upsilon+\frac{1}{2})) \quad (3.35)$$

which gives (Prudnikov, A. P., 1983, p. 720)

$$\Gamma(\mathrm{n}+2\upsilon+1)=(2(\upsilon+\frac{1}{2}))_n\Gamma(2(\upsilon+\frac{1}{2})) \quad (3.36)$$

where $(.)_n$ denotes that

$$(2(\upsilon+\frac{1}{2}))_n=\frac{\Gamma(\mathrm{n}+2\upsilon+1)}{\Gamma(2\upsilon+1)}. \quad (3.37)$$

The following identify [38]

$$\Gamma(2\mathrm{z})=\frac{2^{2z-1}}{\sqrt{\pi}}\Gamma(\mathrm{z})\Gamma(\mathrm{z}+\frac{1}{2}) \quad (3.38)$$

is used with Eq. (3.36) and

$$\Gamma(\mathrm{n}+2\upsilon+1)=(2(\upsilon+\frac{1}{2}))_n\Gamma(\upsilon+\frac{1}{2}) .\Gamma(\upsilon+1)\frac{2^{2(\upsilon+\frac{1}{2})-1}}{\sqrt{\pi}} \quad (3.39)$$

is obtained. By substituting Eq. (3.39) into Eq. (3.25) and considering that $n=0$ with $\upsilon=-1/2$ for the electric current

$$F_e(\beta)\Big|_{n=0}=\pi\ f_0^e J_0(\xi\beta) \quad (3.40)$$

is derived. Here, the following equality is being taken into account

$$\Gamma(\mathrm{n}+2\upsilon+1)\Big|_{n=0}=\Gamma(\upsilon+\frac{1}{2}) .\Gamma(\upsilon+1)\frac{2^{2(\upsilon+\frac{1}{2})-1}}{\sqrt{\pi}} \quad (3.41)$$

and the analysis gives the complete expression for the electric current density

$$F_e(\beta)=\pi\ f_0^e J_0(\xi\beta) +2\pi\sum_{n=1}^{\infty}\frac{f_n^e}{n}(-\mathrm{i})^n J_n(\xi\beta) \quad (3.42)$$

for any value of n.

3.2. System of Linear Algebraic Equations for f_n^e

In the previous section, the Fourier transform of $\tilde{f}_e(\zeta)$ for $\upsilon=-\dfrac{1}{2}$ was obtained as

$$F_e(\beta)=\pi\sum_{n=0}^{\infty}X_nJ_n(\xi\beta) \tag{3.43}$$

where

$$X_n=f_0^e \quad for \quad n=0 \tag{3.44}$$

and

$$X_n=2(-\mathrm{i})^n\frac{f_n^e}{n} \quad for \quad n\neq 0. \tag{3.45}$$

If Eq. (3.43) is substituted into Eq. (2.47), the problem is reduced to that of finding the unknowns f_n^e with $n=0,1,2,...$ as follows:

$$\eta\pi\sum_{n=0}^{\infty}X_nJ_n(\xi\beta)=4\sqrt{1-\cos^2\theta_0}\,\frac{\sin\xi(\beta+\cos\theta_0)}{\xi(\beta+\cos\theta_0)} -\frac{1}{\pi}\int_{-\infty}^{\infty}\frac{\sqrt{1-t^2}\,\sin\xi(\mathrm{t}-\beta)}{\mathrm{t}-\beta}\left\{\pi\sum_{n=0}^{\infty}X_nJ_n(\xi t)\right\}dt. \tag{3.46}$$

By rearranging Eq. (3.46)

$$\eta\pi\sum_{n=0}^{\infty}X_nJ_n(\xi\beta)=+4\sqrt{1-\cos^2\theta_0}\,\frac{\sin\xi(\beta+\cos\theta_0)}{\xi(\beta+\cos\theta_0)} -\sum_{n=0}^{\infty}X_n\int_{-\infty}^{\infty}\frac{\sqrt{1-t^2}\,\sin\xi(\mathrm{t}-\beta)}{\mathrm{t}-\beta}J_n(\xi t)dt \tag{3.47}$$

is obtained. In order to be able to express Eq. (3.47) in a more convenient form for numerical calculations, both sides of the equations will be multiplied by

$$\frac{J_{l+\tau}(\xi\beta)}{\beta^\tau} \quad for \quad l=0,1,2...$$

and by integrating each term with respect to β from $-\infty$ *to* ∞

$$\eta\pi\int_{-\infty}^{\infty}\frac{J_{l+\tau}(\xi\beta)}{\beta^\tau}\sum_{n=0}^{\infty}X_nJ_n(\xi\beta)\,\mathrm{d}\beta= 4\int_{-\infty}^{\infty}\sqrt{1-\cos^2\theta_0}\,\frac{\sin\xi(\beta+\cos\theta_0)}{\xi(\beta+\cos\theta_0)}\frac{J_{l+\tau}(\xi\beta)}{\beta^\tau}d\beta -\int_{-\infty}^{\infty}\frac{J_{l+\tau}(\xi\beta)}{\beta^\tau}\sum_{n=0}^{\infty}X_n \cdot\int_{-\infty}^{\infty}\frac{\sqrt{1-t^2}\,\sin\xi(\mathrm{t}-\beta)}{\mathrm{t}-\beta}J_n(\xi t)dtd\beta \tag{3.48}$$

is written. If Eq. **Pogreška! Izvor reference nije pronađen.** is rearranged by changing the order of integration and summation, it yields

$$\eta\pi\sum_{n=0}^{\infty}X_n\int_{-\infty}^{\infty}\frac{J_{l+\tau}(\xi\beta)J_n(\xi\beta)}{\beta^\tau}\mathrm{d}\beta= 4\int_{-\infty}^{\infty}\frac{\sqrt{1-\cos^2\theta_0}}{\xi}\frac{\sin\xi(\beta+\cos\theta_0)}{\beta+\cos\theta_0}\frac{J_{l+\tau}(\xi\beta)}{\beta^\tau}\mathrm{d}\beta -\sum_{n=0}^{\infty}X_n\int_{-\infty}^{\infty}\sqrt{1-t^2}J_n(\xi t)\left\{\int_{-\infty}^{\infty}\frac{\sin\xi(\mathrm{t}-\beta)}{\mathrm{t}-\beta}\frac{J_{l+\tau}(\xi\beta)}{\beta^\tau}d\beta\right\}dt. \tag{3.49}$$

The integrals in the first and second terms on the right-hand side of Eq. (3.49) can be calculated as follows from the equality given in [38]:

$$\frac{1}{\pi}\int_{-\infty}^{\infty}\frac{J_{l+\tau}(\xi\beta)}{\beta^\tau}\frac{\sin\xi(\mathrm{t}-\beta)}{\mathrm{t}-\beta}d\beta=\frac{J_{l+\tau}(\xi t)}{t^\tau}. \tag{3.50}$$

This equality will give the value of the first integral on the right-hand side of Eq. (3.49) by setting $t=-\cos\theta_0$ which yields

$$\frac{1}{\pi}\int_{-\infty}^{\infty}\frac{J_{l+\tau}(\xi\beta)}{\beta^\tau}\frac{\sin\xi(\beta+\cos\theta_0)}{\beta+\cos\theta_0}d\beta= \frac{J_{l+\tau}(-\xi\cos\theta_0)}{(-\cos\theta_0)^\tau}. \tag{3.51}$$

By using the series representation of Bessel functions, the negative argument functions can be expressed as follows in terms of Bessel functions with positive arguments:

$$\frac{1}{\pi}\int_{-\infty}^{\infty}\frac{J_{l+\tau}(\xi\beta)}{\beta^\tau}\frac{\sin\xi(\beta+\cos\theta_0)}{\beta+\cos\theta_0}d\beta= (-1)^l\frac{J_{l+\tau}(\xi\cos\theta_0)}{\cos^\tau\theta_0}. \tag{3.52}$$

Now, substitution of Eq. (3.50), Eq. (3.51) into Eq. (3.49) yields that,

$$\eta\sum_{n=0}^{\infty}X_n\int_{-\infty}^{\infty}\frac{J_{l+\tau}(\xi\beta)J_n(\xi\beta)}{\beta^\tau}\mathrm{d}\beta= \frac{4\sqrt{1-\cos^2\theta_0}}{\xi}(-1)^l\frac{J_{l+\tau}(\xi\cos\theta_0)}{\cos^\tau\theta_0} -\sum_{n=0}^{\infty}X_n\int_{-\infty}^{\infty}\frac{J_{l+\tau}(\xi t)}{t^\tau}J_n(\xi t)\sqrt{1-t^2}dt. \tag{3.53}$$

The integral on the left-hand side of Eq. (3.53) is denoted as

$$d_{\mathrm{ln}}^{E1}=\int_{-\infty}^{\infty}\frac{J_{l+\tau}(\xi\beta)J_n(\xi\beta)}{\beta^\tau}\mathrm{d}\beta \tag{3.54}$$

and the integral on the right hand side is named as

$$D_{\mathrm{ln}}^{E1}=\int_{-\infty}^{\infty}\frac{J_{l+\tau}(\xi t)J_n(\xi t)}{t^\tau}\sqrt{1-t^2}dt \tag{3.55}$$

So, by substituting these two equations into Eq. (3.53)

$$\eta\sum_{n=0}^{\infty}X_nd_{\mathrm{ln}}^{E1}=\lambda^{E1}-\sum_{n=0}^{\infty}X_nD_{\mathrm{ln}}^{E1} \tag{3.56}$$

is obtained with

$$\lambda^{E1}=-\frac{4\sqrt{1-\cos^2\theta_0}}{\xi}(-1)^l\frac{J_{l+\tau}(\xi\cos\theta_0)}{\cos^\tau\theta_0}. \tag{3.57}$$

Now Eq. (3.56) can be arranged simply as

$$\lambda^{E1} = \sum_{n=0}^{\infty} X_n(\eta d_{\ln}^{E1} + D_{\ln}^{E1}) \tag{3.58}$$

which gives an infinite system of linear algebraic equations for f_n^e. The details of the numerical computation will be shown in the following sections which requires to manipulate analytically the integral seen above.

3.3. System of Linear Algebraic Equations for f_n^m

In the previous section, the Fourier transform of $\tilde{f}_m(\zeta)$ for $\upsilon = \frac{1}{2}$ was obtained as,

$$F_m(\beta) = \pi \sum_{n=0}^{\infty} Y_n \frac{J_{n+1}(\xi\beta)}{\xi\beta} \tag{3.59}$$

where

$$Y_n = (-\mathrm{i})^n(\mathrm{n}+1)\, f_n^m. \tag{3.60}$$

If this equation is substituted into Eq. (2.46)

$$\begin{aligned}-\frac{1}{\xi\eta}\pi\sum_{n=0}^{\infty} Y_n \frac{J_{n+1}(\xi\beta)}{\xi\beta} &= 4i\frac{\sin\xi(\beta+\cos\theta_0)}{\xi(\beta+\cos\theta_0)} \\ &+\frac{1}{\xi\pi}\int_{-\infty}^{\infty}\frac{\sin\xi(\mathrm{t}-\beta)}{(t-\beta)\sqrt{1-t^2}}\left\{\pi\sum_{n=0}^{\infty} Y_n\frac{J_{n+1}(\xi t)}{\xi t}\right\}dt\end{aligned} \tag{3.61}$$

is obtained. By changing the order of integration and summation and by rearranging the equation

$$\begin{aligned}-\frac{\pi}{\eta}\sum_{n=0}^{\infty} Y_n \frac{J_{n+1}(\xi\beta)}{\xi\beta} &= 4i\frac{\sin\xi(\beta+\cos\theta_0)}{(\beta+\cos\theta_0)} \\ &+\sum_{n=0}^{\infty} Y_n\left\{\int_{-\infty}^{\infty}\frac{\sin\xi(\mathrm{t}-\beta)}{(t-\beta)\sqrt{1-t^2}}\frac{J_{n+1}(\xi t)}{\xi t}dt\right\}\end{aligned} \tag{3.62}$$

is written. By multiplying both sides of Eq. (3.62) by $\beta^{-1}J_{l+1}(\xi\beta)$ and integrating each term with respect to β from $-\infty$ to ∞

$$\begin{aligned}-\frac{\pi}{\eta}\int_{-\infty}^{\infty}\left\{\frac{J_{l+1}(\xi\beta)}{\beta}\sum_{n=0}^{\infty} Y_n\frac{J_{n+1}(\xi\beta)}{\xi\beta}\right\}d\beta &= \\ 4i\int_{-\infty}^{\infty}\frac{\sin\xi(\beta+\cos\theta_0)}{(\beta+\cos\theta_0)}\frac{J_{l+1}(\xi\beta)}{\beta}d\beta \\ +\int_{-\infty}^{\infty}\frac{J_{l+1}(\xi\beta)}{\beta}\sum_{n=0}^{\infty} Y_n\left\{\int_{-\infty}^{\infty}\frac{\sin\xi(\mathrm{t}-\beta)}{(t-\beta)\sqrt{1-t^2}}\frac{J_{n+1}(\xi t)}{\xi t}dt\right\}d\beta\end{aligned} \tag{3.63}$$

is found. Or

$$\begin{aligned}-\frac{\pi}{\eta}\sum_{n=0}^{\infty} Y_n\int_{-\infty}^{\infty}\frac{1}{\xi}\frac{1}{\beta^2}J_{l+1}(\xi\beta)J_{n+1}(\xi\beta)d\beta &= \\ 4i\int_{-\infty}^{\infty}\frac{\sin\xi(\beta+\cos\theta_0)}{(\beta+\cos\theta_0)}\frac{J_{l+1}(\xi\beta)}{\beta}d\beta \\ +\sum_{n=0}^{\infty} Y_n\int_{-\infty}^{\infty}\left\{\frac{J_{n+1}(\xi t)}{\xi t}\frac{1}{\sqrt{1-t^2}}\int_{-\infty}^{\infty}\frac{\sin\xi(\mathrm{t}-\beta)}{(t-\beta)}\frac{J_{l+1}(\xi\beta)}{\beta}d\beta\right\}dt.\end{aligned} \tag{3.64}$$

Each term in Eq. (3.64) will be written later in a form more convenient for numerical calculations. For using similar notations with the previous section

$$d_{\ln}^{E2} = \int_{-\infty}^{\infty}\frac{J_{n+1}(\xi\beta)J_{l+1}(\xi\beta)}{\beta^2}\mathrm{d}\beta \tag{3.65}$$

is written. Now to evaluate the integral on the right-hand side of Eq.(3.64), Eq. (3.50) is used with $\tau = 1$, and $t = -\cos\theta_0$ which gives

$$\frac{1}{\pi}\int_{-\infty}^{\infty}\frac{J_{l+1}(\xi\beta)}{\beta}\frac{\sin\xi(\beta+\cos\theta_0)}{\beta+\cos\theta_0}d\beta = \frac{J_{l+1}(-\xi\cos\theta_0)}{-\cos\theta_0}. \tag{3.66}$$

By substituting, Eq. (3.66) into Eq. (3.64)

$$\begin{aligned}-\frac{\pi}{\eta\xi}\sum_{n=0}^{\infty} d_{\ln}^{E2}Y_n &= 4i\frac{J_{l+1}(-\xi\cos\theta_0)}{-\cos\theta_0}\pi \\ &+\sum_{n=0}^{\infty} Y_n\int_{-\infty}^{\infty}\frac{J_{n+1}(\xi\,\mathrm{t})J_{l+1}(\xi\,\mathrm{t})\pi}{\xi\,\mathrm{t}\,\sqrt{1-t^2}\,\,t}dt\end{aligned} \tag{3.67}$$

is obtained, or

$$-\frac{1}{\eta}\sum_{n=0}^{\infty} d_{\ln}^{E2}Y_n = \lambda^{E2} + \sum_{n=0}^{\infty} Y_n D_{\ln}^{E2} \tag{3.68}$$

is written, where

$$D_{\ln}^{E2} = \int_{-\infty}^{\infty} J_{n+1}(\xi\,\mathrm{t})J_{l+1}(\xi\,\mathrm{t})\frac{1}{t^2\sqrt{1-t^2}}dt \tag{3.69}$$

$$\lambda^{E2} = 4i(-1)^l\xi\frac{J_{l+1}(\xi\cos\theta_0)}{\cos\theta_0}. \tag{3.70}$$

Finally, Eq. (3.68) can be expressed as,

$$-\lambda^{E2} = \sum_{n=0}^{\infty} Y_n\left(\frac{1}{\eta}d_{\ln}^{E2} + D_{\ln}^{E2}\right) \tag{3.71}$$

which is the system of linear algebraic equations for f_n^m

4. FIELD ANALYSIS

The total field expression Eq. (2.16) involving the electric and magnetic current densities as unknowns is the fundamental formula for field analysis. In the present section, first the field analysis will be presented in a formal way by assuming that the current densities are known. Then, the steps for numerical determination of the unknowns will be given.

4.1. Scattered Far Field and Total Scattering Cross Section

As stated in Eq. (2.5), the scattered field expression was given as

$$\begin{aligned}H_z(x,y) &= H_z^i(x,y) \\ &+\frac{1}{4}\int_{-a}^{a}\left\{kYI_m(x') - iI_e(x')\frac{\partial}{\partial y}\right\}. \\ &H_0^{(1)}\left(k\sqrt{(x-x')^2+y^2}\right)dx.\end{aligned}$$

In order to obtain the scattered far field, the first step is to substitute the asymptotic expression of Hankel for large argument. Which is given as [5, p.337]

$$H_n^{(1)}(\mathrm{z}) \approx \sqrt{\frac{2}{\pi z}}e^{i(z-\frac{2n+1}{4}\pi)}. \tag{4.1}$$

Using

$$x = r\cos\varphi, \quad y = r\sin\varphi \tag{4.2}$$

in the following expression which is a part of the argument of the Hankel function:

$$\begin{aligned}(\mathrm{x}-\mathrm{x}')^2 + y^2 &= r^2\cos^2\varphi - 2r\,\mathrm{x}'\cos\varphi + \mathrm{x}'^2 + r^2\sin^2\varphi \\ &= r^2 - 2r\,\mathrm{x}'\cos\varphi + \mathrm{x}'^2\end{aligned} \tag{4.3}$$

or

$$(\mathrm{x}-\mathrm{x}')^2 + y^2 = r^2(1 - 2\frac{\mathrm{x}'}{r}\cos\varphi + (\frac{\mathrm{x}'}{r})^2),$$

is written. Then, by inserting it into the argument

$$\begin{aligned}k\sqrt{(\mathrm{x}-\mathrm{x}')^2 + y^2} &= kr\sqrt{1 - 2\frac{\mathrm{x}'}{r}\cos\varphi + (\frac{\mathrm{x}'}{r})^2} \\ &= kr\sqrt{1 - 2\frac{\mathrm{kx}'}{kr}\cos\varphi + (\frac{\mathrm{kx}'}{kr})^2}\end{aligned} \tag{4.4}$$

and by using the binomial expansion formula

$$\begin{aligned}k\sqrt{(\mathrm{x}-\mathrm{x}')^2 + y^2} &= kr\left\{1 - \frac{\mathrm{kx}'}{kr}\cos\varphi + O(\frac{1}{(\mathrm{kr})^2})\right\} \\ &= kr(1 - \frac{\mathrm{x}'}{r}\cos\varphi) + O(\frac{1}{\mathrm{kr}}).\end{aligned} \tag{4.5}$$

is obtained. So as $kr \to \infty$ Eq. (3.2) can be expressed as,

$$\begin{aligned}H_0^{(1)}(k\sqrt{(\mathrm{x}-\mathrm{x}')^2 + y^2}) &\approx H_0^{(1)}(kr(1 - \frac{\mathrm{x}'}{r}\cos\varphi)) \\ &= \sqrt{\frac{2}{\pi kr}}(1 - \frac{\mathrm{x}'}{r}\cos\varphi)^{-\frac{1}{2}} e^{i\left\{kr(1-\frac{\mathrm{x}'}{r}\cos\varphi)-\frac{\pi}{4}\right\}}\left\{1 + O(\frac{1}{\mathrm{kr}})\right\}\end{aligned} \tag{4.6}$$

and by rearranging simply

$$\begin{aligned}H_0^{(1)}(k\sqrt{(\mathrm{x}-\mathrm{x}')^2 + y^2}) &= \\ \sqrt{\frac{2}{i\pi kr}} e^{i(kr(1-\frac{\mathrm{x}'}{r}\cos\varphi))}&\left\{1 + O(\frac{1}{\mathrm{kr}})\right\}\end{aligned} \tag{4.7}$$

is written. If Eq. (4.7) is substituted into the equation of scattered field the following is obtained

$$\begin{aligned}H_z^s(x,y) &= H_z^s(\mathrm{r},\varphi) = \\ -\frac{i}{4}\sqrt{\frac{2}{i\pi kr}} e^{ikr} &\int_{-a}^{+a}\left\{f_1(x') + f_2(x')\frac{\partial}{\partial y}\right\} e^{-ik\,\mathrm{x}'\cos\varphi} dx'.\end{aligned} \tag{4.8}$$

The following of the partial derivative in polar coordinates

$$\frac{\partial}{\partial y} = \frac{\partial r}{\partial y}\frac{\partial}{\partial r} + \frac{\partial\varphi}{\partial y}\frac{\partial}{\partial\varphi} \tag{4.9}$$

with Eq. (4.2)

$$\frac{\partial}{\partial y} = \sin\varphi\frac{\partial}{\partial r} + \frac{\cos\varphi}{r}\frac{\partial}{\partial\varphi} \tag{4.10}$$

and considering for large r, the second term on the right-hand side is obviously zero. So, Eq. (4.8) can be written as

$$\begin{aligned}H_z^s(\mathrm{r},\varphi) &= -\frac{i}{4}\sqrt{\frac{2}{i\pi kr}} e^{ikr} \\ \cdot\int_{-1}^{+1}&\left\{\tilde{f}_1(\zeta') + \frac{\xi\sin\varphi}{4}\tilde{f}_2(\zeta')\right\} e^{-i\xi\zeta'\cos\varphi} d\zeta'.\end{aligned} \tag{4.11}$$

Then, let the scattered field be expressed as

$$H_z^s(\mathrm{r},\varphi) = A(\mathrm{kr})\phi(\varphi) \tag{4.12}$$

where,

$$A(\mathrm{kr}) = \sqrt{\frac{2}{\pi kr}} e^{i(kr-\frac{\pi}{4})} \tag{4.13}$$

and,

$$\phi(\varphi) = \phi_e(\varphi) + \phi_m(\varphi). \tag{4.14}$$

In this case $\phi(\varphi)$ represents the far field radiation pattern. The integrals in Eq. (4.11) are the Fourier transforms of the current density functions. By using Eq. (3.43) and Eq. (3.59) the $\phi_e(\varphi)$ and $\phi_m(\varphi)$ can be obtained as follows:

$$\phi_e(\varphi) = \frac{\pi}{4}\sum_{n=0}^{\infty} X_n J_n(\xi\cos\varphi) \tag{4.15}$$

and,

$$\phi_m(\varphi) = \frac{\xi\sin\varphi}{4}\pi\sum_{n=0}^{\infty} Y_n \frac{J_{n+1}(\xi\cos\varphi)}{\xi\cos\varphi}. \tag{4.16}$$

As known the total scattering cross section can be calculated as [5, p.102],

$$\frac{\sigma_s}{4a} = -\frac{1}{\xi}\mathrm{Re}\left\{\phi(\theta)\right\} \tag{4.17}$$

where θ is the incident angle. It is obvious that the calculation of the RCS requires to know the values of X_n and Y_n. From the analysis accomplished in the previous sections, it should be clear that the determination of X_n and Y_n is reduced to numerical evaluation of $D_{\ln}^{E1}, D_{\ln}^{E2}, d_{\ln}^{E1}$ and $d_{\ln}^{E2}$.

5. NUMERICAL ANALYSIS

As shown in the previous section the analysis of the scattered field is reduced to the numerical evaluation of the functions $d_{\ln}^{E_{1,2}}$ and $D_{\ln}^{E_{1,2}}$. The integral expressions of these terms given by equations Eq. (3.54), Eq. (3.55), Eq. (3.65), and Eq. (3.69) are not convenient for numerical calculations. Therefore by using some analytical methods these integrals are evaluated as follows:

$$d_{ln}^{E_1} = \frac{1}{\xi}\left(\frac{\xi}{2}\right)^{\tau} \cdot \frac{\left[1+(-1)^{l+n}\right]\Gamma(\tau)\Gamma\left(\frac{n+l+1}{2}\right)}{\Gamma\left(\frac{n-l+1}{2}\right)\Gamma\left(\frac{l-n+1+2\tau}{2}\right)\Gamma\left(\frac{n+l+2\tau+1}{2}\right)}. \tag{5.1}$$

$$d_{ln}^{E_2}=\frac{8\xi\left(-1\right)^{\frac{n-l}{2}}}{\pi\left(n+l+3\right)\left(n+l+1\right)\left\{1-\left(n-l\right)^2\right\}} \tag{5.2}$$

$$\begin{aligned}
D_{ln}^{E_1}=&\left\{1+\left(-1\right)^{l+n}\right\}\left\{\frac{\xi^{l+n+\lambda+\tau}}{4}\sum_{k=0}^{\infty}h_{kln}^{\lambda,\tau}\xi^{2k}\frac{\Gamma\left(k+\frac{l+n}{2}+\frac{1}{2}\right)}{\Gamma\left(k+\frac{l+n}{2}+2\right)}\right\}\\
&i.\{\sum_{k=-1}^{\frac{l+n}{2}-1}\frac{1}{4\pi}\frac{\Gamma\left(-k+\frac{l+n}{2}\right)\Gamma\left(k+\frac{1}{2}\right)\Gamma\left(k+\frac{\lambda+\tau+1}{2}\right)}{\Gamma\left(k+2\right)\Gamma\left(k-\frac{l+n}{2}+l+\tau+1\right)}\\
&\times\frac{\Gamma\left(k+\frac{\lambda+\tau}{2}+1\right)}{\Gamma\left(k+\frac{l+n}{2}+\lambda+\tau+1\right)\Gamma\left(k-\frac{l+n}{2}+n+\lambda+1\right)}e^{2k+\lambda+\tau}\\
&-\sum_{k=0}^{\infty}\frac{1}{4\pi}\frac{\Gamma\left(k+\frac{l+n+1}{2}\right)}{\Gamma\left(k+\frac{l+n}{2}+2\right)}h_{kln}^{\lambda,\tau}e^{2k+l+n+\lambda+\tau}\times\left\{2\ln\xi+\psi\left(k+\frac{l+n+1}{2}\right)\right.\\
&+\psi\left(k+\frac{l+n+\lambda+\tau+1}{2}\right)+\psi\left(k+\frac{l+n+\lambda+\tau}{2}+1\right)-\psi\left(k+1\right)\\
&-\psi\left(k+\frac{l+n}{2}+2\right)-\psi\left(k+l+\tau+1\right)\\
&\left.-\psi\left(k+n+\lambda+1\right)-\psi\left(k+l+n+\lambda+\tau+1\right)\right\}\}
\end{aligned} \tag{5.3}$$

$$\begin{aligned}
D_{ln}^{E_2}=&\left\{1+\left(-1\right)^{l+n}\right\}\{R_{ln1}^{E_2}\left(\tau,\lambda\right)=\\
&\frac{\xi^{l+n+\lambda+\tau}}{2}\sum_{k=0}^{\infty}h_{kln}^{\lambda,\tau}\xi^{2k}\frac{\Gamma\left(k+\frac{l+n}{2}+\frac{1}{2}\right)}{\Gamma\left(k+\frac{l+n}{2}+1\right)}\}\\
&-i\{\sum_{k=0}^{\frac{l+n}{2}-1}\frac{1}{2\pi}\frac{\Gamma\left(-k+\frac{l+n}{2}\right)\Gamma\left(k+\frac{1}{2}\right)\Gamma\left(k+\frac{\lambda+\tau+1}{2}\right)}{\Gamma\left(k+1\right)\Gamma\left(k-\frac{l+n}{2}+n+\lambda+1\right)}\\
&\times\frac{\Gamma\left(k+\frac{\lambda+\tau}{2}+1\right)}{\Gamma\left(k+\frac{l+n}{2}+\lambda+\tau+1\right)\Gamma\left(k-\frac{l+n}{2}+l+\tau+1\right)}\\
&.e^{2k+\lambda+\tau}W_n\\
&-\sum_{k=0}^{\infty}\frac{1}{2\pi}\frac{\Gamma\left(k+\frac{l+n+1}{2}\right)}{\Gamma\left(k+\frac{l+n}{2}+1\right)}h_{kln}^{\lambda,\tau}e^{2k+l+n+\lambda+\tau}\\
&\quad\times\left\{2\ln\xi+\psi\left(k+\frac{l+n+1}{2}\right)\right.\\
&+\psi\left(k+\frac{l+n+\lambda+\tau+1}{2}\right)+\psi\left(k+\frac{l+n+\lambda+\tau}{2}+1\right)\\
&-\psi\left(k+1\right)\\
&-\psi\left(k+\frac{l+n}{2}+1\right)-\psi\left(k+l+\tau+1\right)\\
&\left.-\psi\left(k+n+\lambda+1\right)-\psi\left(k+l+n+\lambda+\tau+1\right)\right\}\}
\end{aligned} \tag{5.4}$$

where,

$$W_n=0,\qquad l+n=0$$

$$W_n=1,\qquad \mathrm{l+n}\neq 0.$$

$\Gamma(.)$ denotes the Gamma function and,

$$h_{kln}^{\lambda\tau}=\left(-1\right)^k .\frac{\Gamma\left(k+\frac{l+n+\lambda+\tau+1}{2}\right)\Gamma\left(k+\frac{l+n+\lambda+\tau+2}{2}\right)}{\Gamma\left(k+1\right)\Gamma\left(k+l+n+\lambda+\tau+1\right)\Gamma\left(k+n+\lambda+1\right)\Gamma\left(k+l+\tau+1\right)}. \tag{5.5}$$

6. RESULTS

The approach method used in this thesis is a hybrid method named as analytical-numerical method. In general, the aim of using hybrid methods is to eliminate the disadvantages of the analytical methods which operate well at high frequencies and of the numerical methods which operate well at low frequencies. Stated in other words its aim is, to obtain an accurate solution for a wide frequency range. By comparing the results obtained by Veliev et al. [51] and the ones obtained by using this method it can be easily concluded that our results are much close to results obtained by Veliev et al. [51]. Figure 6.1, Figure 6.2, Figure 6.3, and Figure 6.4 illustrate the monostatic RCS as a function of incidence angle for *ka* = 5.0, 15.0. In order to investigate the effect of the surface impedance on the scattered far field, two different cases have been considered as in η = 1.5 and η=3.0. In view of the two RCS curves for the impedance strip, the backscattered field is not affected by the impedance of the strip surface in the shadow region. On the other hand, Figure 6.5, Figure 6.6, Figure 6.7, and Figure 6.8 illustrate the bistatic RCS as a function of observation angle for θ = 60° and *ka* = 5.0, 15.0. It is seen from the figures that our RCS results agree quite well with the results of Veliev et al. [51]. In addition, there are different trials in Figure 6.9 - Figure 6.15.

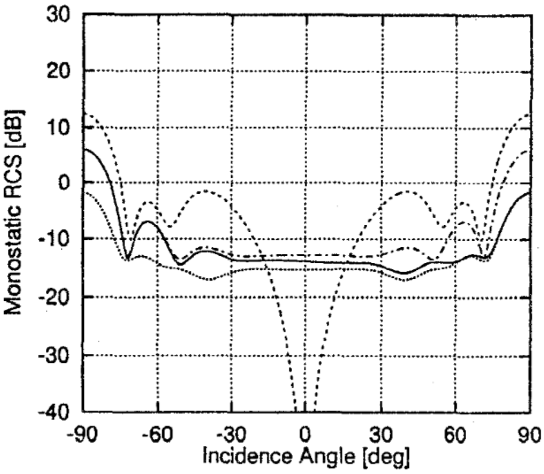

Figure 6.1. Monostatic RCS [dB], $\theta_0 = 60^o$, *ka* = 5.0.
$- - - -$: $\eta_1 = \eta_2 = 0.0$; ——— : $\eta_1 = 1.5,\ \eta_2 = 3.0$;
.... : $\eta_1 = \eta_2 = 1.5$; -.-.-.- : $\eta_1 = \eta_2 = 3.0$
(Veliev et al. [51])

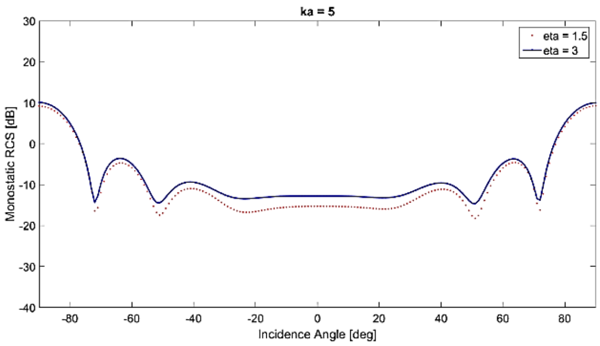

Figure 6.2. Monostatic RCS [dB], ka=5.0
$(\eta = 1.5 and\ \eta = 3.0)$

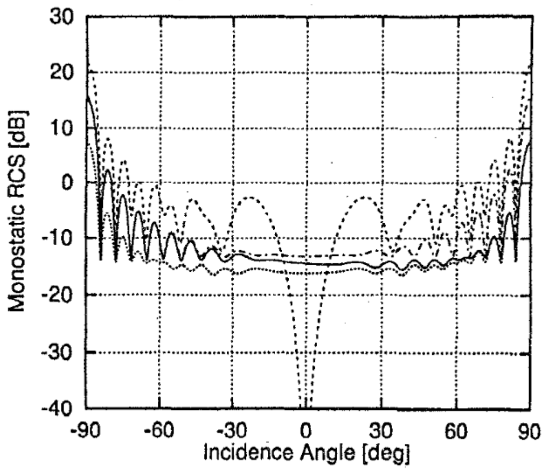

Figure 6.3. Monostatic RCS [dB], $\theta_0 = 60^o$, *ka*=15.0.
$- - - -$: $\eta_1 = \eta_2 = 0.0$; ——— : $\eta_1 = 1.5,\ \eta_2 = 3.0$;
.... : $\eta_1 = \eta_2 = 1.5$; -.-.-.- : $\eta_1 = \eta_2 = 3.0$
(Veliev et al. [51])

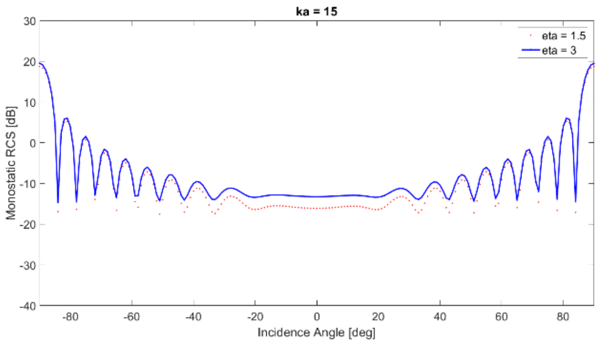

Figure 6.4. Monostatic RCS [dB], *ka*=15.0
$(\eta = 1.5 and\ \eta = 3.0)$

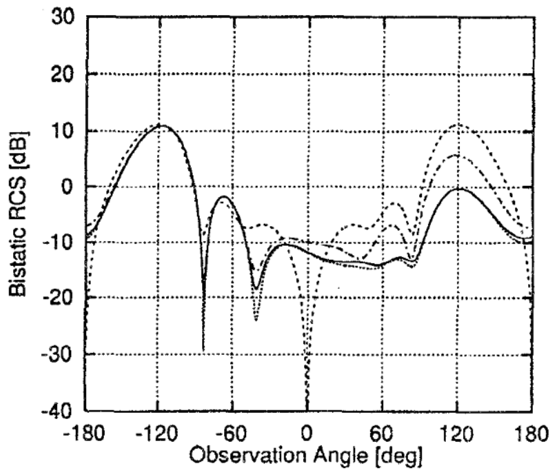

Figure 6.5. Bistatic RCS [dB], $\theta_0 = 60^o$, *ka*=5.0.
$- - - -$: $\eta_1 = \eta_2 = 0.0$; ——— : $\eta_1 = 1.5,\ \eta_2 = 3.0$;
.... : $\eta_1 = \eta_2 = 1.5$; -.-.-.- : $\eta_1 = \eta_2 = 3.0$
(Veliev et al. [51])

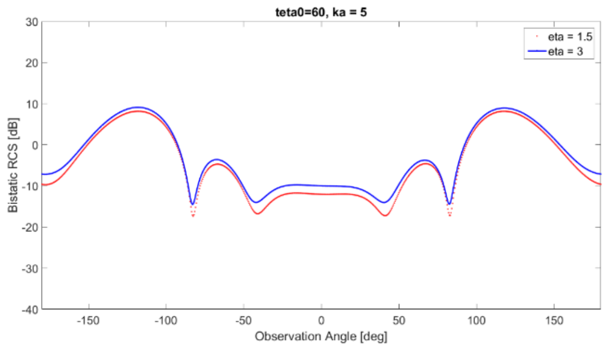

Figure 6.6. Bistatic RCS [dB], *ka*=5.0
$(\eta = 1.5 \, and \, \eta = 3.0)$

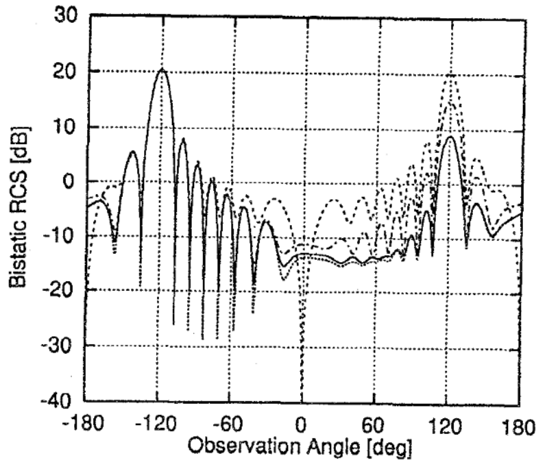

Figure 6.7. Bistatic RCS [dB], $\theta_0 = 60^o$, *ka*=15.0.
- - - - : $\eta_1 = \eta_2 = 0.0$; ——— : $\eta_1 = 1.5, \ \eta_2 = 3.0$;
.... : $\eta_1 = \eta_2 = 1.5$; - · - · - : $\eta_1 = \eta_2 = 3.0$
(Veliev et al. [51])

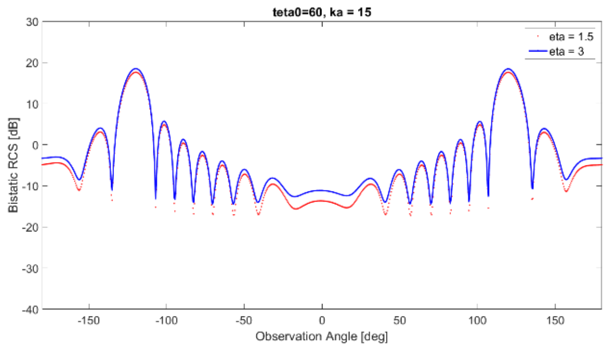

Figure 6.8. Bistatic RCS [dB], *ka*=15.0
$(\eta = 1.5 \, and \, \eta = 3.0)$

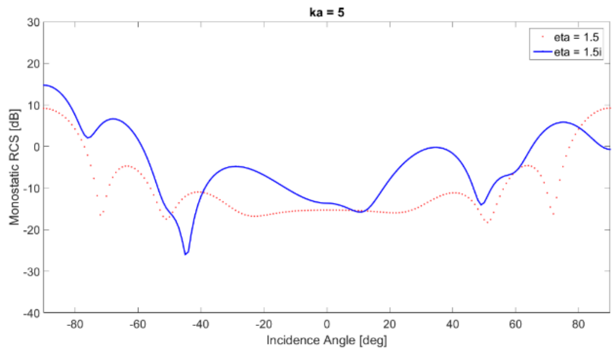

Figure 6.9. Monostatic RCS [dB], *ka*=5.0
$(\eta = 1.5 \, and \, \eta = 1.5i)$

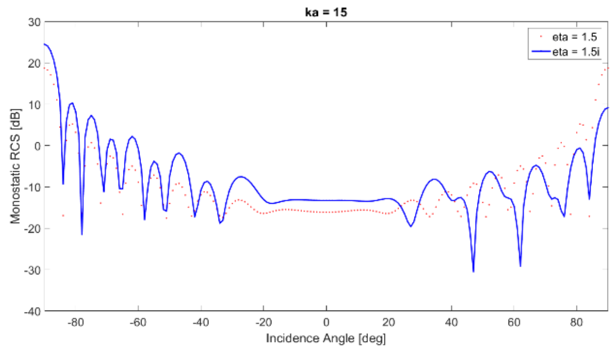

Figure 6.10. Monostatic RCS [dB], ka=15.0
$(\eta = 1.5 \, and \, \eta = 1.5i)$

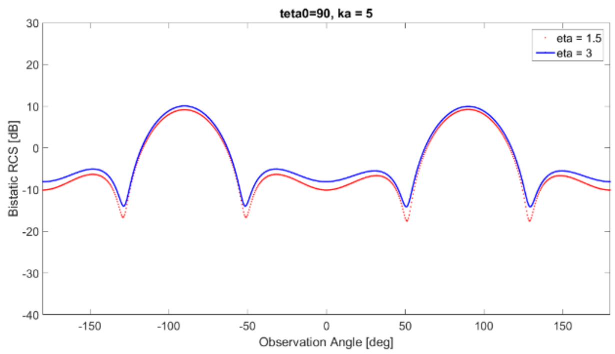

Figure 6.11. Bistatic RCS [dB], $\theta_0 = 90^{\circ}$, ka=5.0
$(\eta = 1.5 \, and \, \eta = 3.0)$

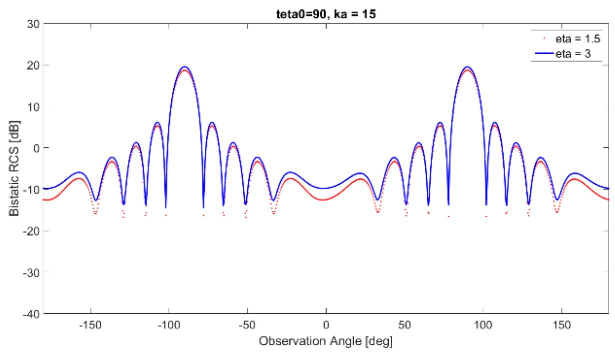

Figure 6.12. Bistatic RCS [dB], $\theta_0 = 90^{\circ}$, *ka*=15.0
$(\eta = 1.5 \, and \, \eta = 3.0)$

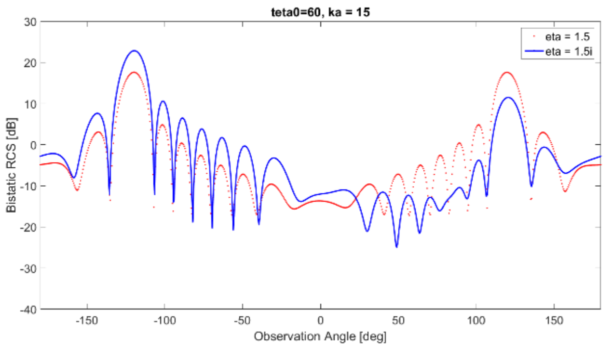

Figure 6.13. Bistatic RCS [dB], $\theta_0 = 60^\circ$, *ka*=15.0 $(\eta = 1.5 \text{ and } \eta = 1.5i)$

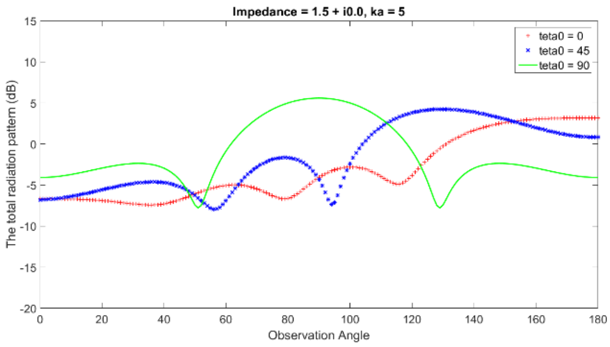

Figure 6.14. The total radiation pattern for *ka*=5

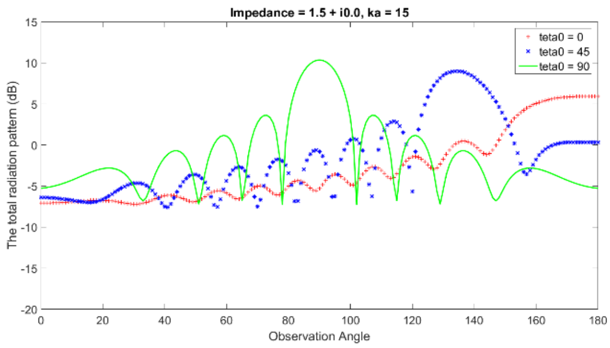

Figure 6.15. The total radiation pattern for *ka*=15

7. CONCLUSION

In this study, the diffraction of the H-polarized plane wave by an infinitely long strip, having the same impedance on both faces with a width of 2*a* is considered. Applying the boundary condition to an integral representation of the scattered field, the problem is formulated as simultaneous integral equations satisfied by the electric and magnetic current density functions. The integral equations are reduced to two uncoupled infinite systems of linear algebraic equations and physical quantities are obtained in terms of the solution of systems of linear algebraic equations. Numerical examples on the monostatic radar cross section (RCS), bistatic RCS, and the total scattering field radiation pattern are presented. Some obtained results are compared with the other existing results.

The system which is considered in this thesis is the simple impedance strip illuminated normally by a plane wave. The canonical strip structure is chosen in terms of its conformity to many practical problems. This method is applicable for the analysis of more complicated structures which may be considered as a combination of different strip configurations. At that rate, the mathematical sense of the solution will not change. However, there will be some extra terms in the matrix equations. Because of this, the computer codes in this thesis must be modified for different strip configurations.

8. REFERENCES

[1] Abramowitz, M.; Stegun, I. E., 1968. Handbook of Mathematical Functions. Dower Publications, New York, p. 1043.

[2] Ahluwalia, D. S., 1970. Uniform Asymptotic Theory of Diffraction by the Edge of a Three-Dimensional Body. SIAM J. Appl. Math. Vol.18, No.2, pp. 287-301.

[3] Apaydin, G.; Sevgi, L., 2015. Method of Memonts Modeling of Backscattering By a Soft-Hard Strip. IEEE Trans. on Atennas and Propagation, Vol.63, No.12, pp. 5822-5826.

[4] Bhattacharyya, A. K.; Sengupta, D. L., 1991. Radar Cross Section Analysis and Control. Artech House, London, p. 289. (Uffimtsev, P. I., 1958).

[5] Born, M.; Wolf, E., 1965. Principles of Optics. Pergamon Press, Frankfurt, Germany, p.808. (Rayleigh, L., 1871).

[6] Bowman, J. J., 1967. High-Frequency Backscattering from an Absorbing Infinite Strip with Arbitrary Face Impedance. Canadian Journal of Phys., Vol. 45, pp. 2409-2430.

[7] Burnside, W. D.; Yu, C. L.; Marhefka, R. J., 1975. A Technique to Combine the Geometrical Theory of Diffraction and the Moment Method. IEEE Trans. On Ant. And Proc., Vol. AP-23, pp. 551-558.

[8] Butler, C. M., 1985. General Solution of the Narrow Strip Integral Equations. IEEE Trans. on Ant. and Proc., Vol. AP-33, No. 10, pp. 1085-1090.

[9] Büyükaksoy, A.; Serbest, A. H.; Uzgören, G., 1989. Secondary Diffraction of Plane Waves by an Impedance Strip. Radio Science, Vol. 24, pp. 455-464.

[10] Castro, L. P.; Kapanadze, D., 2008. The impedance boundary value problem of diffraction by a strip. J. Math. Appl., Vol. 337, pp. 1031-1040.

[11] Chakrabarti, A., 1977. Diffraction by a uni-directionally conducting strip. Ind. J. Pure Appl. Math., Vol. 8, pp. 702-717.

[12] Copson, E. T., 1946. An integral-equation method of solving plane diffraction problems. Proceedings of the Royal Society A Mathematical, Physical and Engineering Sciences, pp. 100-118.

[13] Emets, V.; Rogowski, J., 2015. Diffraction by a Strip with Different Boundary Condtions on Its Surfaces. 16th International Conference on Computational Problems of Electrical Engineering (CPEE), Lviv (Ukraine), pp. 39-42.

[14] Faulkner, T. R., 1965. Diffraction of an Electromagnetic Plane-wave by a Metallic Strip.

IMA Journal of Applied Mathematics, Vol. 1, pp. 149-163.
[15] Felsen, L. B.; Marcuvitz, N., 1973. Radiation and Scattered of Waves. Prentice Hall, New Jersey, p. 883.
[16] Grinberg, G. A., 1960. Diffraction of Electromagnetic Waves by Strip of Finite Width. Soviet Phys. Dokland. Vol. 4, No. 6, pp. 1222-1225.
[17] Harrington, R. F., 1968. Field Computation by Moment Method. Macmillan, New York, p. 285.
[18] Herman, M. I.; Volakis, J. L., 1987. High Frequency Scattering by a Resistive Strip and Extensions to Conductive and Impedance Strips. Radio Science, Vol. 22, No. 3, pp. 335-349.
[19] Hongo, K., 1972. Diffraction of Electromagnetic Plane Wave by an Infinite Slit Embedded in an Anisoropic Plasma. Journal of Applied Phyisics, Vol. 43, No. 12, pp. 4996-5001.
[20] Imran, A.; Naqvi, Q. A.; Hongo, K., 2009. Diffraction of electromagnetic plane wave by an infinitely long conducting strip on dielectric slab. Opt Comm, Vol. 282, pp. 443–450.
[21] Imran, A.; Naqvi, Q. A.; Hongo, K., 2007. Diffraction of electromagnetic plane wave by an impedance strip. Prog In Elec Res., Vol. 75, pp. 303–318.
[22] Jones, D. S., 1964. The Theory of Electromagnetism, Pergamon, London.
[23] Keller, J. B., 1962. J. Opt. Soc. Of America, Vol. 52, No. 2, pp. 116-130. (Keller, J. B., 1953).
[24] Kouyoumjian, R. G.; Pathak, P. H., 1974. A Uniform Geometrical Theory of Diffraction for Edge in a Perfect Conducting Surface. Proc. Of the IEEE, Vol. 62, No. 11, pp. 1448-1461.
[25] Kobayashi, K., 1993. The Wiener-Hopf Technique and Its Applications to Diffraction problems Involving Two Dimensional Obstacles with Finite Cross-Section. Lecture Notes, p. 145.
[26] Lawrie, J. B.; Abrahams, I. D., 2007. A brief historical perspective of the Wiener-Hopf technique. J. Eng. Math., Vol. 59, pp. 351-358.
[27] Levine, H.; Schwinger, J., 1948. On the Theory of Electromagnetic Wave Diffraction by an Aperture in an Infinite Plane Conducting Screen. Comm. Pure and Appl. Math., Vol. 3, pp. 355-391.
[28] Maliuzhinets, G. D., 1958. Excitation, Reflection and Emission of Surface Waves from a Wedge with given Face Impedance. Soviet Phys. Dokland, Vol. 3, No. 3, pp. 752-755.
[29] Medgyesi, L. N.; Wang, D. S., 1989. Hybrid Solutions for Scattering from Perfectly Conducting Bodies of Revolution. IEEE Trans. on Antennas and Propagation, Vol. AP-31, No. 4, pp. 570-583.
[30] Medgyesi, L. N.; Wang, D. S., 1989. Hybrid Methods for Analysis of Complex Scatterers. Proc. of the IEEE, Vol. 77, No. 5, pp. 770-779.
[31] Meixner, J., 1972. The Behavior of Electromagnetic Fields at Edges. IEEE Trans. on Ant. and Prop. Vol. AP-20, No. 4, pp. 442-446. (Meixner, J., 1949).
[32] Miles, J. W., 1949. On Certain Integral Equations in Diffraction Theory. Vol. 28, pp. 223-226.
[33] Morse, P. M.; Rubenstein, P. J., 1938. The Diffraction of Waves by Ribbons and Slits. Phys. Rev., Vol. 54, pp. 895-898.
[34] Nagasaka, T.; Kobayashi, K., 2015. Wiener-Hopf Analysis of the Plane Wave Diffraction by a Thin Material Strip: the Case of H-polarization. Electromagnetics in Advanced Applications (ICEAA) 2015 International Conference, Turin, pp. 626-628.
[35] Noble, B., 1958. Methods Baesd on the Wiener-Hopf Technique. Pergamon, London.
[36] Nomura, Y.; Katsura, S., 1957. Diffraction of Electromagnetic Waves by Circular Plate and Circular Hole. J. Phys. Soc. Japan, Vol. 10, No. 4, pp. 285-304.
[37] Otsuki, T., 1978. Diffraction by two parallel slits in plane. J. Math. Phys., Vol. 46, pp. 911-915.
[38] Prudnikov, A. P.; Brickov, Y. A.; Maricev, O. I., 1983. Integrals and Series of Special Functions. Nauka Press, Moskow, p. 785.
[39] Rayleigh, L., 1871. On the scattering of light by small particles. Philosophical Magazine, series 4, Vol. 41, pp. 447-454.
[40] Spiegel, M. R., 1968. Mathematical Handbook of Formulas and Tables. Mc-Graw Hill Company, New York, p. 271.
[41] Sahalos, J. N.; Thiele, G. A., 1981. On the Application of the GTD-MM Technique and Its Limitations. IEEE Trans. on Ant. and Proc., Vol. AP-29, pp. 780-786.
[42] Senior, T. B. A., 1951. Diffraction by a Semi-Infinite Metallic Sheet. Proc. of the Royal Society, Vol. 213, pp. 436-458.
[43] Senior, T. B. A., 1979. Backscattering from Resistive Strips. IEEE Trans. on Ant. and Proc., Vol. AP-27, No. 6, pp. 808-813.
[44] Serbest, A. H.; Büyükaksoy, A., 1993. Some Approximate Methods Related to the Diffraction by Strips and Slits. Analytical and Numerical Methods in Electromagnetic Wave Theory, Science House, Japan, pp. 229-256.
[45] Sommerfeld, A., 1896. Mathematische Theorie der Diffraction. Math. Ann. 47, pp. 317-374.
[46] Thiele, G. A.; Newhouse, T. H., 1975. A Hybrid Technique for Combining Moment Method with the Geometrical Theory of Diffraction. IEEE Trans. on Ant. and Proc., Vol. AP-23, Jan., pp. 62-69.
[47] Tiberio, R.; Kouyoumjian, R. G., 1979. A Uniform GTD Solution for the Diffraction by Strips Illuminated at Grazing Incidence. Radio Science, Vol. 14, No. 6, pp. 933-941.
[48] Veliev, E. I.; Kobayashi, K.; Ogata, M., Koshikawa, S., 1998. Diffraction by a Strip with Different Surface Impedances: The Case of H Polarization. VII International Conference on Mathematical Methods in Electromagnetic Theory, Vol. 2, pp. 727-729.
[49] Veliev, E. I.; Veremey, V. V., 1993. Numerical-Analytical Approach for the Solution to the Wave Scattering by Polygonal Cylinders and Flat Strip Structures. M. Hashimoto, M. İdemen, O.A. Tretyakov. Analytical and Numerical Methods in

Electromagnetic Wave Theory, Science House, Japan, pp. 471-514.
[50] Veliev, E. I.; Veremey, V. V.; Shestopalov, V. P., 1989. Electromagnetic Wave Diffraction on Polygonal Cylinders-New Approach. Proc. of 1989 URSI Int. Symp. on Electromagnetic Theory, p. 628.
[51] Veliev, E. I.; Kobayashi, K.; Ogata, M., 1998. Diffaction by a strip with different surface impedances: the case of H polarization. Proceedings of 1998 International Conference on MMET, Kharkov, Ukraine, pp. 727-730.
[52] Volakis, J. L.; Bindiganavale, S. S., 1996. Scattering by a Narrow Groove in an Impedance Plane. Radio Science, Vol. 31, No. 2, pp. 401-408.
[53] Wandzura, S., 1992. Electrical Current Basis Functions for Curved Surfaces. Electromagnetics, Vol. 12, Np. 1, pp. 77-90.

Contact addresses

Emine Avşar Aydin, Assistant Professor
Adana Science and Technology University, Department of Aeronautics Engineering
Seyhan/Adana-TURKEY
+90-05318436781
eaydin@adanabtu.edu.tr / rasvaenime@gmail.com

Turgut İkiz, Professor
Çukurova University, Department of Electrical-Electronic Engineering
Adana-TURKEY
+90-03223386868
tikiz@cu.edu.tr